Journal of Vertebrate Paleontology

ISSN: (Print) (Online) Journal homepage: www.tandfonline.com/journals/ujvp20

First record of *Borealosuchus sternbergii* from the lower Paleocene Denver Formation (lower Danian), Colorado (Denver Basin)

Emily J. Lessner, Holger Petermann & Tyler R. Lyson

To cite this article: Emily J. Lessner, Holger Petermann & Tyler R. Lyson (09 Jan 2025): First record of *Borealosuchus sternbergii* from the lower Paleocene Denver Formation (lower Danian), Colorado (Denver Basin), Journal of Vertebrate Paleontology, DOI: 10.1080/02724634.2024.2434214

To link to this article: https://doi.org/10.1080/02724634.2024.2434214

Journal of Vertebrate Paleontology e2434214 (21 pages)

DOI: 10.1080/02724634.2024.2434214

ARTICLE

FIRST RECORD OF *BOREALOSUCHUS STERNBERGII* FROM THE LOWER PALEOCENE DENVER FORMATION (LOWER DANIAN), COLORADO (DENVER BASIN)

EMILY J. LESSNER, [1,2]* HOLGER PETERMANN,[1] and TYLER R. LYSON[1]
[1]Denver Museum of Nature & Science, Department of Earth Sciences, Denver, Colorado 80205, U.S.A.;
[2]Bureau of Land Management, Moab, Utah 84532, U.S.A.

ABSTRACT—The Late Cretaceous through Paleogene fossil record for North American eusuchians is remarkable in that it indicates high levels of survivorship across the Cretaceous–Paleogene (K–Pg) boundary, as well as an increase in diversity through the early Eocene. Despite the clade's continued existence, gaps remain in its fossil record, particularly near the K–Pg boundary and in Colorado. A eusuchian from the lower Paleocene Denver Formation of Corral Bluffs is represented by specimens identified as *Borealosuchus sternbergii*. Here, we provide anatomical descriptions and comparisons supported by micro-CT scan data of three partial crania. We conduct a phylogenetic analysis, the results of which are influenced by the potential sub-adult ontogenetic stage of the specimens and species-level assignment is preliminary. The specimens fill both geographic and temporal gaps in the record of the *Borealosuchus* species complex as the first specimens from the earliest Paleocene of Colorado. These additions highlight the uncertainty in phylogenetic relationships among the *Borealosuchus* species complex, the importance of taking ontogenetic stage into account when assessing such relationships, and help constrain biogeographic dispersal patterns and ecological niche occupation of the clade.

SUPPLEMENTARY FILES— Supplementary files are available for this article for free at www.tandfonline.com/UJVP

Citation for this article: Lessner, E. J., Petermann, H., & Lyson, T. R. (2025) First record of *Borealosuchus sternbergii* from the lower Paleocene Denver Formation (lower Danian), Colorado (Denver Basin). *Journal of Vertebrate Paleontology*. https://doi.org/10.1080/02724634.2024.2434214

Submitted: January 15, 2024
Revisions received: November 14, 2024
Accepted: November 15, 2024

INTRODUCTION

Eusuchia is a clade of neosuchian crocodylomorphs that first appeared in the Middle–Late Jurassic (De Celis et al., 2020). Whereas the pre-Campanian record is largely represented by European and Asian specimens, the Late Cretaceous saw an increase in North American paleodiversity with the appearance of the *Borealosuchus* species complex and groups such as alligatoroids, gavialoids, and crocodyloids (De Celis et al., 2020). North American eusuchian paleodiversity was not impacted by the Cretaceous–Paleogene (K–Pg) extinction event and species of *Borealosuchus* and alligatoroids were widespread during this time interval (Brochu, 1999; Buffetaut, 1990; Markwick, 1998; MacLeod et al., 1997; Sullivan, 1987). The semi-aquatic behaviors of eusuchians and the members of their food chain likely facilitated survival through the impact event resulting in no impact to their net diversification rate as a result of the K–Pg extinction (Buffetaut, 1990; Markwick, 1998; Robertson et al., 2004). There are, however, a few notable gaps in the eusuchian record during that time. For example, Colorado to date represents a geographic gap between a seeming northern and southern Paleocene radiation of Eusuchia (Brochu, 2000) and a temporal gap between the Late Cretaceous representatives and Paleocene and Eocene taxa. Despite widespread exposure of Late Cretaceous through Eocene sedimentary units in Colorado (Fig. 1), exposure of the K–Pg and the earliest Paleocene is limited.

The sequence of rocks at the Corral Bluffs study area in Colorado Springs spans the K–Pg Boundary and represents the last ~300 thousand years of the Cretaceous and first one-million years of the Paleocene (Lyson et al., 2019). It is unique in its density of localities with remarkably complete vertebrates and flora (Lyson et al., 2019). One such group of vertebrates present are eusuchians, notably specimens morphologically similar to species of *Borealosuchus*, a taxon that is otherwise minimally documented in Colorado (Hester, 2018; McCormack, 2019). *Borealosuchus* is a clade of eusuchians with ambiguous phylogenetic placement, often recovered just inside (e.g., Brochu, 1997, 2004; Brochu et al., 2012; Buscalioni et al., 2011; Delfino et al., 2008; Farke et al., 2014; Martin et al., 2014; Nárvaez et al., 2015; Puértolas et al., 2011; Wu & Brinkman, 2015) or outside (e.g., Figueiredo et al., 2011; McCormack, 2019; Pol et al., 2009; Rio & Mannion, 2021) of Crocodylia. Because of this discrepancy, the clade is important in reconstructing the evolution and distribution of the early members of crown Crocodylia.

The *Borealosuchus* species complex is widespread both geographically and stratigraphically. Species of *Borealosuchus* are known from southern Alberta and Saskatchewan, Canada (Lindblad et al., 2022; Sternberg, 1932; Wu et al., 2001) to Big Bend, Texas (Brochu, 2000) in western North America to New Jersey (Brochu et al., 2012) and Alabama (McCormack, 2019) in eastern North America, and from the Late Cretaceous through

*Corresponding author:
Color versions of one or more of the figures in the article can be found online at www.tandfonline.com/ujvp.

Published online 09 Jan 2025

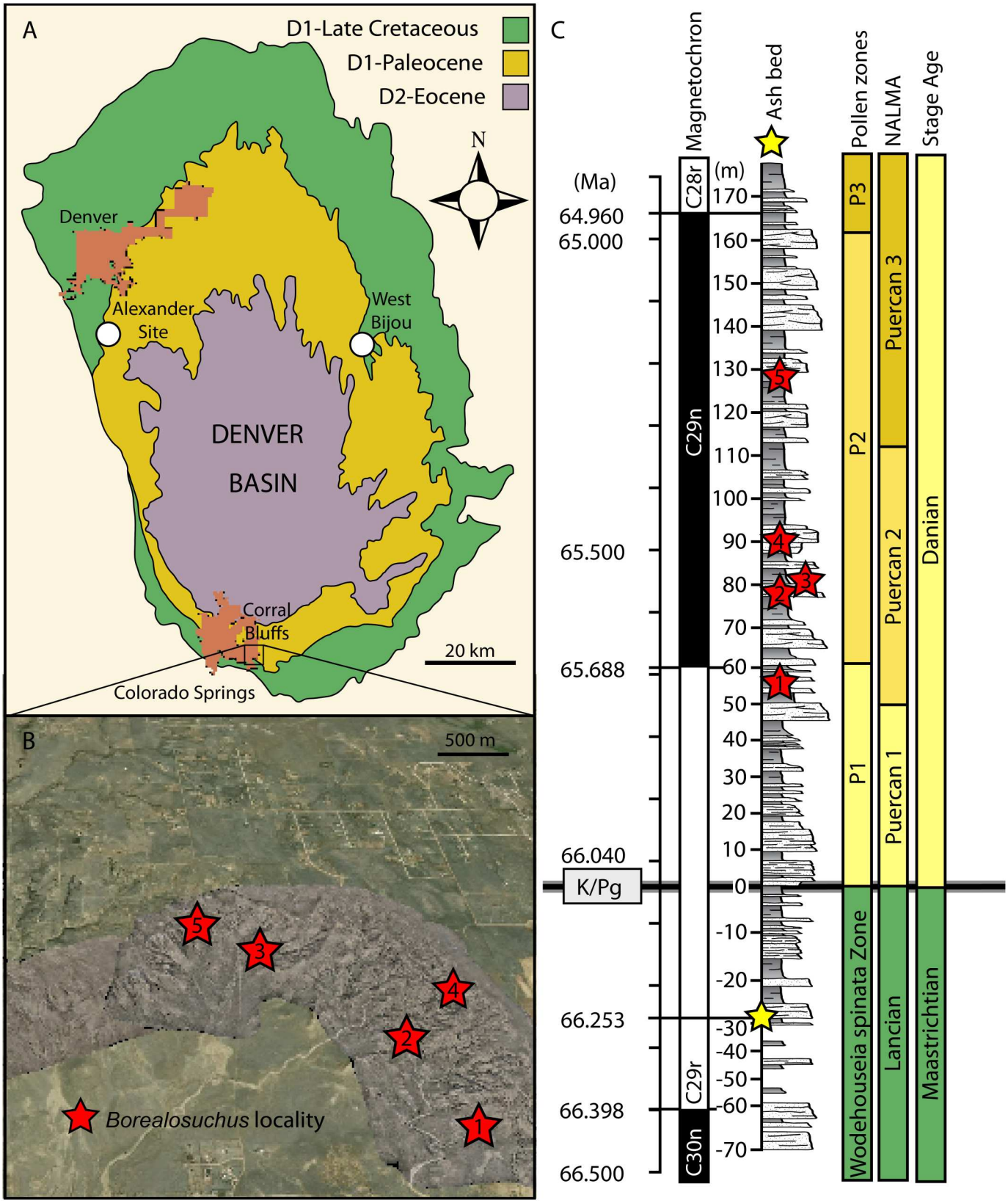

FIGURE 1. Locality placement of *Borealosuchus* specimens. **A**, location of the Corral Bluffs study area, West Bijou, and the Alexander Site within the Denver Basin; **B**, location of *Borealosuchus* localities in the Corral Bluffs study area on a high-resolution photogrammetry model: (1) DMNH EPV.143022/DMNH loc. 6994; (2) DMNH EPV.60862/DMNH loc. 3887; (3) DMNH EPV.144434/DMNH loc. 18840; (4) DMNH EPV.136252/DMNH loc. 7071; (5) UCM 123254/UCM loc. 83196; **C**, magnetostratigraphic, lithostratigraphic, chronostratigraphic and biostratigraphic placement of *Borealosuchus* localities. Modified from Lyson et al. (2021a). **Abbreviations**: **km**, kilometer; **m**, meters; **Ma**, million years ago; **K/Pg**, Cretaceous–Paleogene boundary.

the Eocene. Currently, seven species are recognized for *Borealosuchus* (one without phylogenetic support, *B. griffithi*; Lindblad et al., 2022; Wu et al., 2001), with two species recognized from before the K–Pg boundary (Alabama *Borealosuchus* [McCormack, 2019] and *B. sternbergii* [Gilmore, 1910]), one around the boundary (*B. threeensis* [Brochu et al., 2012]), and four after (*B. formidabilis* [Erickson, 1976], *B. acutidentatus* [Sternberg, 1932], *B. wilsoni* [Mook, 1959], and *B. griffithi* [Lindblad et al., 2022; Wu et al., 2001]).

Here we present three incomplete *Borealosuchus* skulls (DMNH EPV.60862, DMNH EPV.136252, and DMNH EPV.144434), together representing ~70–80% of the cranium and some tentatively referred material. The specimens represented by crania are relatively small and other features indicate a sub-adult ontogenetic stage. Information on growth in members of *Borealosuchus* is limited (Erickson, 1976) so these specimens provide a unique window into ontogeny in the clade. The material represents the first record of *Borealosuchus* from the Denver Basin and is temporally interesting because of the proximity to the K–Pg boundary. We explore phylogenetic context of the Corral Bluffs material and the wider implications for improving the ambiguous phylogenetic placement of the genus *Borealosuchus* within Eusuchia and the evolutionary history of early members of crown-Crocodylia.

GEOLOGICAL SETTING

The material herein described comes from two distinct study areas (Corral Bluffs and West Bijou) in the Denver Basin where the D1 sequence of the Denver Formation is exposed, spanning the uppermost Cretaceous (ca. 67 Ma) through the lower Paleocene (ca. 65 Ma [Lyson et al., 2019]; Fig. 1). The D1 sequence is composed of reworked Mesozoic and Paleozoic sediments as well as Precambrian basement rock shed during the Laramide uplift of the Front Range (Hagadorn et al., 2023; Raynolds, 2002; Raynolds & Johnson, 2003). The Corral Bluffs study area is located east of Colorado Springs, El Paso County, Colorado, U.S.A. in the southwestern portion of the Denver Basin. The area is located ~39N, is distal to the Western Interior Seaway, and is proximal (~2–20 km) to the Rocky Mountain Front Range. The south-facing arc, or "corral," of exposure that makes up the Corral Bluffs Study area is the most extensive outcropping of the D1 sequence in the Denver Basin (Raynolds, 2002). The Denver Formation in this area is characterized by alternating fine to coarse arkosic sandstones, drab silty mudstones, and laminated siltstones, which are all characteristic of a higher-energy fluvial depositional environment where perennially high-water tables resulted in pond and hydromorphic soil formation (Fuentes et al., 2019; Lyson et al., 2019). The West Bijou study area, situated ~75 km to the north and east of the Corral Bluffs study area, is located in Arapahoe and Elbert counties in the eastern portion of the Denver Basin (Fig. 1). This area is dominated by lignites interspersed with fine-grained sandstones and drab mudstones, which reflect a low-energy fluvial depositional environment where perennially high-water tables led to formation of swamps, lakes, and hydromorphic soils (Barclay et al., 2003; Raynolds, 2002).

The Corral Bluffs study area has produced hundreds of remarkably complete vertebrates, including turtles (Lyson et al., 2019, 2021a, 2021b), mammals (Bertrand et al., 2022; Krause et al., 2021; Weaver et al., 2024), and crocodilians (Lyson et al., 2019). The deposit is shallowly buried (Petermann et al., 2022) and many of the fossils are preserved in phosphatic concretions, a mode of preservation that is highly unusual for a terrestrial environment (Lyson et al., 2019). The material herein described was found as disassociated float on the East side of the arc of south-facing cliffs that is Corral Bluffs (Fig. 1B). DMNH EPV.60862 is an unconcreted specimen that was found at the base of a ridge in a coarse-grained, mustard-colored sandstone unit interpreted to represent a fluvial channel deposit. The tentatively referred UCM 123254, DMNH EPV.143024, DMNH EPV. 67785, and DMNH EPV.67756 were found as float in a similar deposit. DMNH EPV.136252, DMNH EPV.144434, and DMNH EPV.143022 were preserved in fine-grained phosphatic concretions. The specimens were discovered in sediments that represent the Puercan (Pu) II North American Land Mammal Age (NALMA) biostratigraphic zone and pollen biostratigraphic zone 2 (Lyson et al., 2019; Nichols & Fleming, 2002; Fig. 1C). These localities are 52–89.7 m above the palynologically defined K–Pg boundary (Lyson et al., 2019). DMNH EPV.144434 was found *in situ* and whereas DMNH EPV.60862 and 136252 were found as float and their stratigraphic placement and age cannot be precisely determined, it is worth noting that they are relatively complete and likely were not transported far (i.e., likely meters rather than tens of meters) down section (Beardmore et al., 2012; de Araújo & da Silva Marinho, 2013; Grange & Benton, 1996; Salisbury et al., 2003; Schwarz-Wings et al., 2011; Syme & Salisbury, 2014). Thus DMNH EPV.60862 has a stratigraphic placement of 78.9 meters above the palynologically defined K–Pg boundary and estimated age of 65.56 Ma, DMNH EPV.136252 has a stratigraphic placement of 89.7 meters above the K–Pg boundary and an estimated age of 65.49 Ma, and DMNH EPV.144434 has a stratigraphic placement of 78.4 meters above the K–Pg boundary and an estimated age of 65.6 Ma (Lyson et al., 2019; Fig. 1C). Given the specimens moved down section, these ages represent maximum age estimates.

The tentatively referred *Borealosuchus* specimens from West Bijou were collected from microvertebrate localities. The specimens were discovered in sediments that represent the Pu I NALMA and pollen biostratigraphic zone 1 (Dahlberg et al., 2016; Nichols & Fleming, 2002; Fig. 1C). These localities are within 5–15 m above the K–Pg boundary with primary indicators of the asteroid impact, including shocked minerals, iridium, and boundary clay (Barclay et al., 2003; Clyde et al., 2016).

METHODS

Preparation

Manual Preparation—Prior to photography, CT scanning, and digital preparation, overlying matrix covering the crania was manually removed using pin vises and air scribes. The fossils were consolidated with Paraloid B72 and cyanoacrylates. Preparation was completed by J. Englehorn, N. Toth, K. Carpenter, S. Bastien, and S. Rush at the Denver Museum of Nature & Science, Denver, CO, U.S.A., as well as contract preparatory S. Begin.

CT Scanning and Digital Preparation—Both DMNH EPV.60862 and DMNH EPV.136252 specimens were scanned at the University of Texas High-Resolution X-Ray CT Facility in March 2023 on an NSI micro-CT scanner. DMNH EPV.60862 was scanned at a voxel size of 49.6 μm at 150 kV, 0.14 mA and DMNH EPV.136252 at a voxel size of 59.4 μm at 170 kV, 0.16 mA. TIFF stacks were imported into ORS Dragonfly version 2022.2 where manual segmentation of cranial elements was completed by E. Lessner using the ROI painter tool and a defined range of grayscale values. CT data and models are available for download from Morphosource (project ID: 000581588).

Body Size Estimation

Trans-quadratic skull width was used as a proxy for body size (as demonstrated by O'Brien et al., 2019). Skull width was measured by hand in DMNH EPV.60862 and DMNH

TABLE 1. Body size (total length and body mass) of *Borealosuchus sternbergii* specimens calculated from trans-quadratic skull width (O'Brien et al., 2019).

Specimen	Skull Width (cm)	Total Length (cm)	Body Mass (kg)	Formation
DMNH EPV.144434	80.0	112.01	3.88	Denver
DMNH EPV.60862	93.7	127.12	6.19	Denver
DMNH EPV.136252	120.9	155.98	13.13	Denver
USNM 6533	184.53	219.02	45.77	Lance
UCMP 133903	190.73	224.909	50.46	Tullock
UCMP 173976	195.76	229.57	54.5	Tullock

EPV.144434. It was estimated for DMNH EPV.136252 by scaling shared elements in the digital model of DMNH EPV.60862 up to the size of the shared elements in DMNH EPV.136252 and measuring the resulting skull width. Other specimens (see Table 1) were measured by hand or from photographs. Both total length and body mass were calculated for DMNH EPV.60862, DMNH EPV.136252, DMNH EPV.144434, USNM 6533, UCMP 133903, and UCMP 173976 using the following equations: $\ln(\text{total length}) = 0.8024(\ln(\text{skull width})) + 3.05$; $\ln(\text{body mass}) = 2.953(\ln(\text{skull width})) - 5.072$.

Phylogenetic Analysis

We investigated the phylogenetic relationships of DMNH EPV.60862, DMNH EPV.136252, and DMNH EPV.144434 using the matrix of McCormack (2019, unpublished MS thesis, see Supplementary Material), itself a modified version of Brochu (2012). The total matrix included 93 taxa and 189 characters and was curated in Mesquite (Maddison & Maddison, 2023; see Supplementary NEXUS files for characters and states). We analyzed the specimens in the Windows version of TNT v.1.6 (Goloboff & Morales, 2023). The updated matrix is included as Supplementary Material. The matrix as created does not include ordered characters, and we did not re-evaluate characters for treatment as ordered. The 'Glen Rose Form' is the outgroup taxon for the analyses. We analyzed the dataset with gentle implied weighting ($k = 12$) as proposed by Goloboff et al. (2018) using New Technology Search. We used 10 drifting cycles in Sectorial Search and set the CSS setting therein to run 10 rounds and set the number of iterations in Drifting to 10. We otherwise used the default settings for Sectorial Search, Ratcheting, Drifting, and Tree Fusing. Using these settings, we required the Minimum Length to be recovered 100 times. Initial analysis of the dataset did not match phylogenetic positions for the modern crocodilians as reported in recent molecular analyses, so we constrained the topology of extant taxa using the molecular framework from Hekkala et al. (2021; see Supplementary TNT files for constraints). This provided a stable framework for the analysis of the fossil taxa. Fossil taxa were allowed to float freely, and we enforced the constraint during all analyses. To increase tree resolution, we then combined DMNH EPV. 60862, 136252, and 144434 into one taxon, 'Denver Basin *Borealosuchus*.' We calculated Bremer supports for the combined analysis (using the Bremer run script with searching 100,000 suboptimal trees and setting the constraints step to search 3 times with constraints and performing10 iterations of 20 ratchet iterations and 20 drifting cycles and doing a monophyly search, but keeping the other settings as default), ran a Bootstrap analysis ($nrep = 2000$), and overlaid those numbers onto the strict consensus tree. We imported the tree file of the resulting MPTs into ASADO 2.0 (formerly WinClada; Nixon, 2021) to read consistency (CI) and retention (RI) indices and to map unambiguous character state changes onto the strict consensus tree.

Three changes were made to the matrix and are detailed in the Supplementary Material. The data matrices for the datasets in which the specimens are scored individually and scored combined are part of the Supplementary Material as NEXUS and as tnt files.

Institutional Abbreviations—**DMNH**, Denver Museum of Nature & Science, Denver, CO, U.S.A.; **NMC**, Canadian Museum of Nature, Ottawa, Ontario, Canada; **SMM**, Science Museum of Minnesota, St. Paul, MN, U.S.A.; **UCM**, University of Colorado Museum, Boulder, CO, U.S.A.; **USNM**, Smithsonian National Museum of Natural History, Washington D.C., U.S.A.

Anatomical Abbreviations—**a**, angular; **bo**, basioccipital; **bs**, basisphenoid; **d**, dentary; **eam**, external auditory meatus; **ect**, ectopterygoid; **emf**, external mandibular fenestra; **ex**, exoccipital; **f**, foramen; **f.ae**, foramen aerum; **f.ca**, foramen for the carotid artery; **f.CNIX + X + vj**, foramen for the glossopharyngeal nerve, vagus nerve, and jugular vein; **f.CNXII**, foramen for the hypoglossal nerve; **f.mag**, foramen magnum; **fos**, fossa; **fr**, frontal; **itf**, infratemporal fenestra; **j**, jugal; **l**, lacrimal; **ls**, laterosphenoid; **mx**, maxilla; **n**, nasal; **nvf**, neurovascular foramen; **op**, occlusion pits; **orb**, orbit; **p.cq**, cranioquadrate passage; **p**, parietal; **pa**, palatine; **pf**, prefrontal; **po**, postorbital; **pr**, prootic; **pt**, pterygoid; **q**, quadrate; **qj**, quadratojugal; **sa**, surangular; **soc**, supraoccipital; **sof**, suborbital fenestra; **sp**, splenial; **sq**, squamosal; **stf**, supratemporal fenestra; **v**, vomer; **V_f**, trigeminal foramen. Anatomical abbreviations follow Lessner & Holliday (2022) where possible.

SYSTEMATIC PALEONTOLOGY

EUSUCHIA Huxley, 1875 (sensu Brochu, 1999)
CROCODYLIA Gmelin, 1789 (sensu Benton & Clark, 1988)
BOREALOSUCHUS Brochu, 1997

Type Species—*Borealosuchus sternbergii* (*Leidyosuchus sternbergii*, Gilmore, 1910), from the Lance Creek Formation (Late Cretaceous) of Wyoming.

Included Species—*Borealosuchus acutidentatus* (Sternberg, 1932) from the terrestrial Ravenscrag Formation (early Paleocene; Puercan) of Saskatchewan, Canada. *Borealosuchus wilsoni* (Mook, 1959) from the terrestrial Green River, Bridger, and Washakie formations (Eocene) of Wyoming. *Borealosuchus formidabilis* (Erickson, 1976) from the terrestrial Tongue River Formation (early Paleocene; Tiffanian 4) of North Dakota. *Borealosuchus threeensis* (Brochu et al., 2012) from the marginal marine Hornerstown Formation (Late Cretaceous/early Paleocene) of New Jersey. *Borealosuchus* sp. nov. (McCormack, 2019) from the marginal marine Mooreville Chalk (Late Cretaceous) of Alabama. Potentially (no phylogenetic support) *Borealosuchus griffithi* (Lindblad et al., 2022; Wu et al., 2001) from the terrestrial Scollard Formation (Late Cretaceous) of Alberta, Canada and the Ravenscrag Formation (early Paleocene; Puercan) of Saskatchewan, Canada.

Original Diagnosis—*Borealosuchus* is diagnosed by Brochu (2000) by: limb bones very long and slender (character 36[1]); surangular extending to posterodorsal end of retroarticular process (character 72[0]); and lateral curvature of the maxillary toothrow posterior to the first six maxillary alveoli (character 94[1]; autapomorphy).

Revised Generic Diagnosis—*Borealosuchus* is diagnosed by atlantal ribs with modest dorsal process on dorsal margin (character 6[0]); the anterior half of axis neural spine slopes anteriorly (character 11[1]); limb bones very long and slender (character 36 [1]; autapomorphy); alveoli for dentary teeth 3 and 4 nearly same

size and confluent (character 47[0]); coronoid with rostrally sloping superior edge (character 56[0]); nasals excluded, at least externally from naris, nasals and premaxillae still in contact (character 82[2]); occlusion pits between 7th and 8th maxillary teeth with all other dentary teeth occluding lingually (character 92[1]); maxillary toothrow curves laterally broadly posterior to first six maxillary alveoli (character 94[1]); large medial jugal foramen (character 102[1]).

BOREALOSUCHUS STERNBERGII Gilmore, 1910 (Figs. 2, 3, 4, 5, and 6)

Type Specimen—USNM 6533, a partial skull with a well-preserved braincase and jaw, eight vertebrae, left and right humeri, right fibula, second left metatarsal, and other fragmentary material.

Type Horizon—Lance Creek Formation.

Synonymy—*Leidyosuchus sternbergii* Gilmore, 1910.

Original Diagnosis—*Leidyosuchus sternbergii* is diagnosed by Brochu (2000) as *Borealosuchus sternbergii* by an enlarged jugal siphonial foramen (character 102[1]).

Revised Specific Diagnosis—Member of *Borealosuchus* with lateral edges of palatines with a lateral process projecting from the palatines into the suborbital fenestra (character 117[1]) and surangular with a spur bordering the dentary tooth row (character 62[0]).

Newly Referred Material from the Denver Formation—The following material is united with *B. sternbergii* on the basis of a concavo-convex frontoparietal suture between the supratemporal fenestrae (character 151[0]), a broad rostral palatine process (character 116[0]), the pterygoid ramus of the ectopterygoid is not straight (character 119[1]), and a lacrimal longer than the prefrontal (character 130[0]).

From Corral Bluffs: DMNH EPV.60862, incomplete caudal skull and fragmentary rostrum consisting of partial quadrates, quadratojugal, maxillae, frontal, parietal, prefrontals, postorbitals, pterygoid, laterosphenoids, prootics, exoccipital, supraoccipital, jugal, basisphenoid, basioccipital, and squamosals (Figs. 2–5); DMNH EPV.136252, central region of skull consisting of prefrontals, lacrimals, vomer, palatines, basisphenoid, basioccipital, prootics, and partial maxillae, nasals, parietal, jugals, ectopterygoids, frontal, postorbitals, squamosals, supraoccipital, pterygoids, laterosphenoids, exoccipitals, quadrates (Figs. 2–4); DMNH EPV.144434, fragmentary skull consisting of ectopterygoids, pterygoid, supraoccipital, exoccipitals, and partial maxillae, palatines, right jugal, right lacrimal, quadrates, squamosals, basioccipital, quadratojugals, and parietal, mandibles consisting of the right dentary, angular, splenial, and partial surangular and left dentary and partial splenial and angular, associated osteoderms, and fragmentary elements including a left humerus and vertebra (Fig. 6).

The following are tentative referrals from Corral Bluffs and West Bijou: UCM 123254, isolated fragment of right maxilla (Fig. S1G–H); DMNH EPV.143022, poorly preserved fragmentary rostrum (Fig. S2); DMNH loc. 143024, isolated osteoderms and vertebra (Fig. S1B, C); DMNH EPV.67785, isolated osteoderms (Fig. S1E); DMNH EPV.67756, isolated osteoderms (Fig. S1F); UCM 110292, isolated osteoderms (Fig. S1A); UCM 63350, isolated osteoderms (Fig. S1D); DMNH EPV.143025, fragmentary cranial material and osteoderms (Fig. S3).

DESCRIPTION AND COMPARISONS

General Skull Features

Both DMNH EPV.136252, 60862, and 144434 are three-dimensionally preserved crania that were found as float and have portions of the skull missing due to erosion. The specimens have dorsal sculpturing, including rounded pitting on the jugals, parietals, caudal frontals, prefrontals, and squamosals (Fig. 2A, C, I, H), though not to the extent of depth present in *Borealosuchus wilsoni* or *Borealosuchus formidabilis*, though poor preservation precludes further description. The preserved lateral margins of DMNH EPV.136252 are linear as are the isolated maxilla fragments of DMNH EPV.60862 (Figs. 2A, D–E, 7). The orbits are large, flush with the surface of the skull, possess a round ventral margin, and narrow rostrally (Figs. 2C, G, H, 7). They are bounded by the lacrimal rostrally, prefrontal and frontal medially, postorbital caudally, and jugal laterally. They resemble those of *B. sternbergii* and *B. griffithi* (Gilmore, 1910; Lindblad et al., 2022; Wu et al., 2001) and are not as round as those of the type specimens of *B. acutidentatus* (NMC 8544) and *B. formidabilis* (SMM P71.16.28; Erickson, 1976; Sternberg, 1932) and are not crescentic as in *B. wilsoni* (Hester, 2018; Fig. 7). The supratemporal fenestrae possess shallow fossae at their rostromedial corner (Fig. 2E) and are circular caudally, but incomplete rostrolateral margins makes determination of the exact shape of the supratemporal fenestrae impossible (Fig. 2A, C, E, G–I). The supratemporal fenestrae are bounded by the parietal rostrally and medially, squamosal caudally and laterally, and postorbital rostrally and laterally, with rostral contribution by the frontal unknown. Where preserved, the bones of the skull roof do not overhang the rim of the supratemporal fenestrae. The infratemporal fenestrae are bounded rostrally by the jugal and postorbital but are otherwise not preserved (Fig. 2C, G, H). In dorsal view, the skull table is concave caudally but the lateral and much of the rostral margins are not preserved (Figs. 2A, E, I, 7). Generally, the skull table appears rectangular though not as broad as that of the Alabama *Borealosuchus*, *B. formidabilis*, and *B. acutidentatus* (Erickson, 1976; McCormack, 2019; Sternberg, 1932; Fig. 7). It is planar dorsally and minimally elevated above the rest of the cranial surface, forming a continuous surface with the rostrum like in other species of *Borealosuchus* (e.g., Erickson, 1976; Gilmore, 1910; Fig. 4). The region rostral to the skull table is smoothly inclined rostrally. The suborbital fenestrae are rostrocaudally elongate as in other species of *Borealosuchus* (Brochu, 1997; Erickson, 1976; Gilmore, 1910; Lindblad et al., 2022; Wu et al., 2001), tapering to a rounded edge rostrally and with a concave caudolateral border (Figs. 3C, G, H, 7). They are bounded by the maxilla rostrally and laterally, palatine medially, pterygoid caudally, and ectopterygoid caudolaterally.

Dorsal Skull Roof

Premaxilla—The premaxilla is only preserved in DMNH EPV.60862 (Fig. 2B). Only the dorsal surface and margins of the external nares are preserved, the ventral surface including alveoli and incisive foramen are missing (and therefore not figured). The element is poorly preserved and crushed to a level that prevents description of its morphology.

Nasal—The nasals of DMNH EPV.136252 are minimally preserved because of the missing rostral extent of the skull (Fig. 2C, G, H). Caudally, they narrow mediolaterally and extend to the junction of the prefrontal and lacrimal though it is not apparent whether the nasal possesses a process between the elements as in *B. griffithi* (Lindblad et al., 2022; Wu et al., 2001). The contact with the frontal is U-shaped and occurs at the rostral extent of the prefrontals to which it extends a short process to the prefrontal rostral tip (2C, G, H).

Maxilla—Dorsally, the maxillae of DMNH EPV.136252 contact the nasals, lacrimals, and jugals (Fig. 2C, G, H). The contact with the nasals is largely missing, though linear at its caudal extent. The caudomedial border of the maxilla is concave where it contacts the rostrolateral edge of the lacrimal

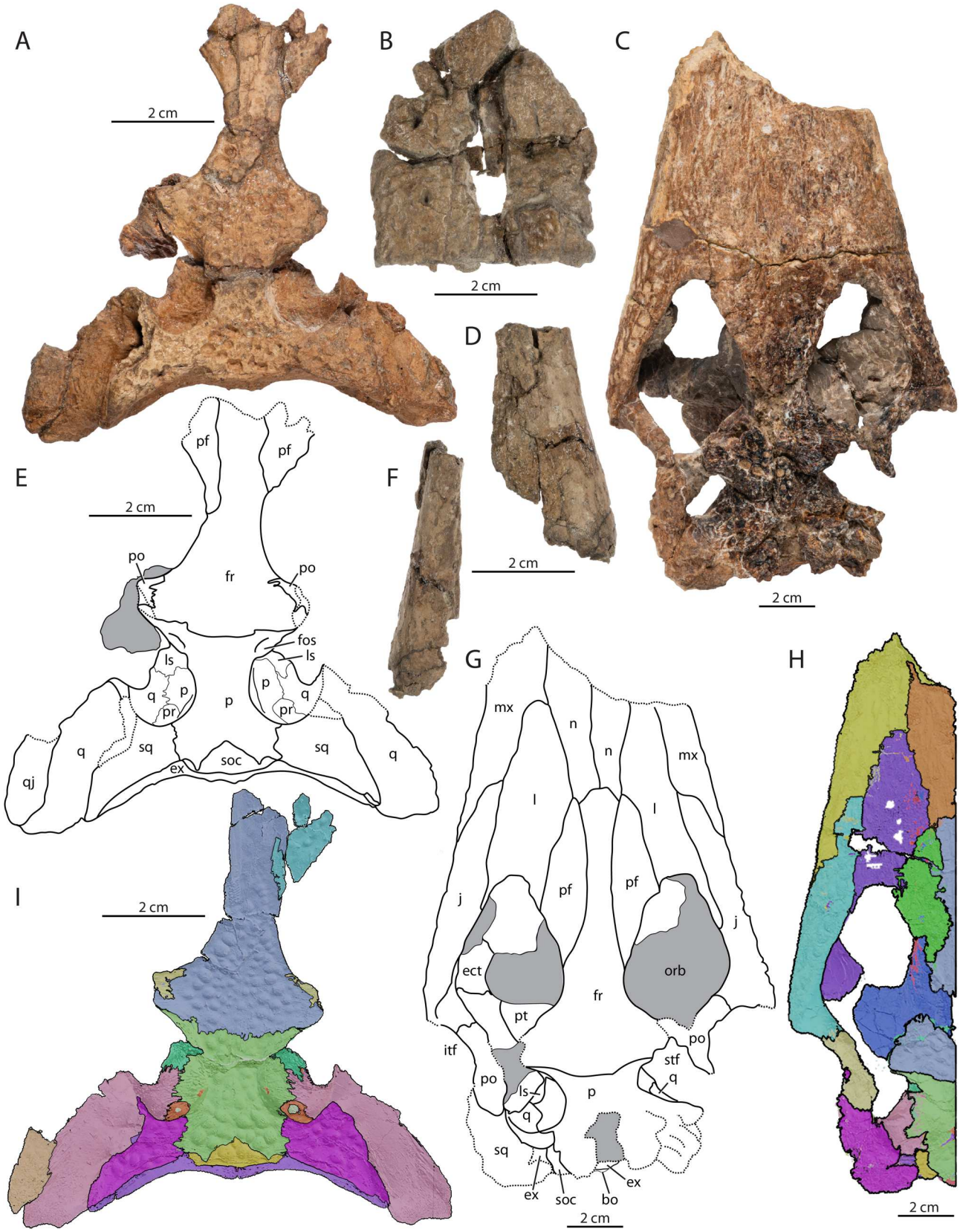

FIGURE 2. Dorsal views of *Borealosuchus sternbergii* fossil material including **A**–**D**, **F**, photographs, **E**,**G**, line drawings, and **H**–**I**, CT reconstructions of **A**, **B**, **D**–**F**, IDMNH EPV.60862, and **C**, **G**, **H**, DMNH EPV.136252. **A**, fragmentary skull; **B**, premaxillary fragment; **C**, fragmentary skull; **D**, right maxilla fragment; **E**, line drawing of **A**; **F**, left maxilla fragment; **G**, line drawing of **C**; **H**, CT reconstruction of **C**; **I**, CT reconstruction of **A**. Dotted lines represent broken surfaces. **Abbreviations**: **bo**, basioccipital; **ect**, ectopterygoid; **ex**, exoccipital; **fos**, fossa; **fr**, frontal; **itf**, infratemporal fenestra; **j**, jugal; **l**, lacrimal; **ls**, laterosphenoid; **mx**, maxilla; **n**, nasal; **orb**, orbit; **p**, parietal; **pf**, prefrontal; **po**, postorbital; **pr**, prootic; **pt**, pterygoid; **q**, quadrate; **qj**, quadratojugal; **soc**, supraoccipital; **sq**, squamosal; **stf**, supratemporal fenestra.

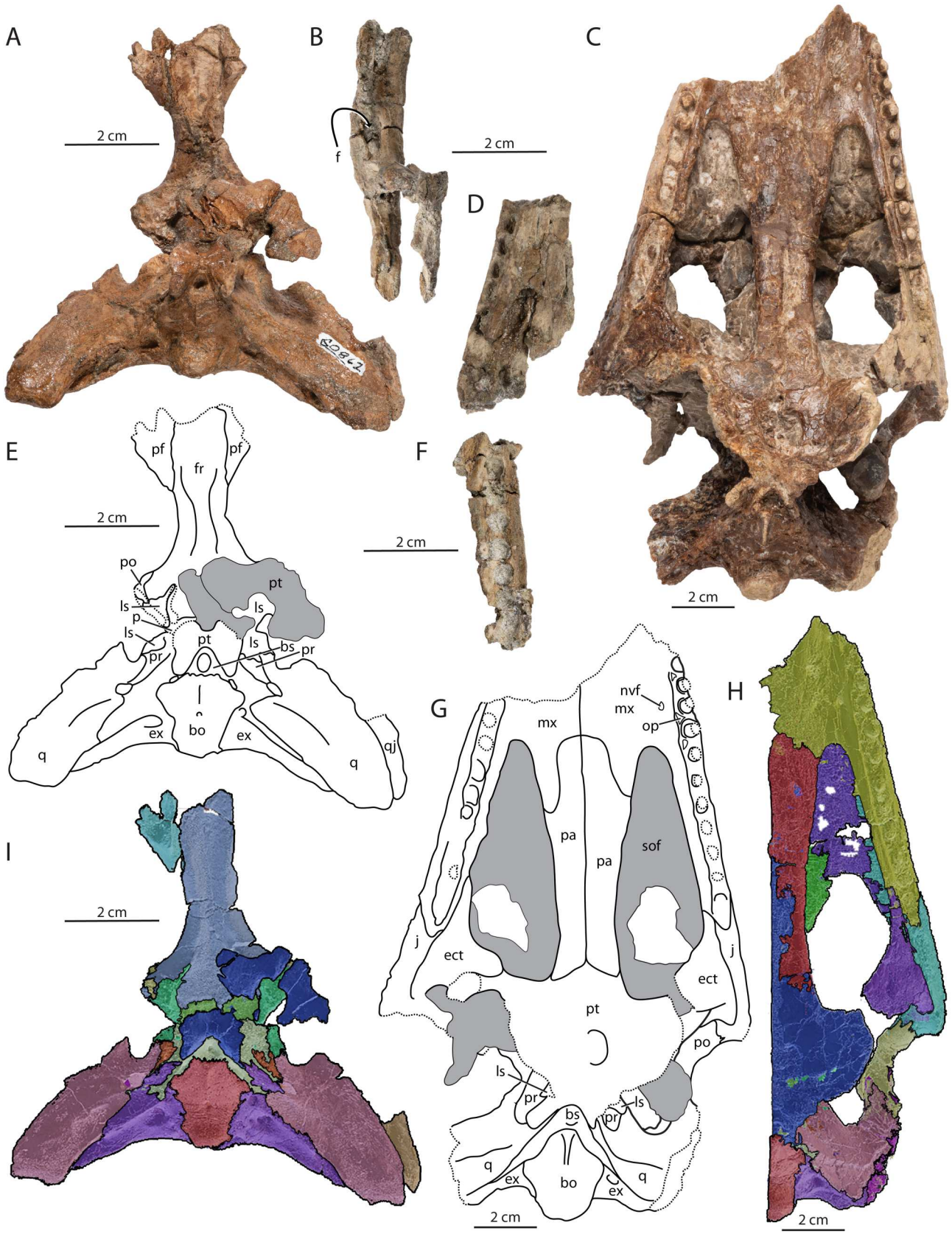

FIGURE 3. Ventral views of *Borealosuchus sternbergii* fossil material including **A**–**D**, **F**, photographs, **E**, **G**, line drawings, and **H**–**I**, CT reconstructions of **A**, **B**, **D**–**F**, **I**, DMNH EPV.60862 and **C**, **G**, **H**, DMNH EPV.136252. **A**, fragmentary skull; **B**, right jugal fragment; **C**, fragmentary skull; **D**, right maxilla fragment; **E**, line drawing of **A**; **F**, left maxilla fragment; **G**, line drawing of **C**; **H**, CT reconstruction of **C**; **I**, CT reconstruction of **A**. Dotted lines represent broken surfaces. **Abbreviations**: **bo**, basioccipital; **bs**, basisphenoid; **ect**, ectopterygoid; **ex**, exoccipital; **f**, foramen; **fr**, frontal; **j**, jugal; **ls**, laterosphenoid; **mx**, maxilla; **nvf**, neurovascular foramen; **op**, occlusion pits; **pa**, palatine; **po**, postorbital; **pr**, prootic; **pt**, pterygoid; **q**, quadrate; **qj**, quadratojugal; **sof**, suborbital fenestra.

(Fig. 2C, G, H). In lateral view, the maxillae extend just caudal to the rostral border of the orbits in a caudoventrally oriented contact with the jugal (Fig. 4A, see Morphosource 3D models). The dorsal surface of the maxilla is unfeatured and linear in lateral view (Fig. 4A). Specimen DMNH EPV 60862 preserves two sections of maxilla with few notable features besides a linear lateral margin (Fig. 2F, D), and poor preservation of DMNH EPV.144434 precludes any description of the dorsal surface of the maxilla besides its linear medial margin (Fig. 6A, B). UCM 123254 preserves several rostral alveoli (likely the third through the sixth), exhibits some lateral expansion, and is upturned rostrally in lateral view (Fig. S1).

Lacrimal—The lacrimal forms the rounded rostromedial and lateral borders of the orbit in DMNH EPV.136252 (Fig. 2C, G, H) and is partially visible in DMNH EPV.144434 (Fig. 6A, B). It is elongate, extending to the 9th alveolus (counted from caudal), and contacts the jugal and maxilla laterally and the nasal and prefrontal medially with a linear margin. The contact with the nasal is not interrupted by a posterior process of the maxilla (Fig. 2C, G, H). The lacrimal tapers rostrally and a slender process extends caudally along the jugal. Overall, it is ovate rostrally in dorsal view similar to *B. griffithi*, *B. sternbergii*, *B. wilsoni*, and *B. acutidentatus* (Gilmore, 1910; Hester, 2018; Sternberg, 1932; Wu et al., 2001; Fig. 7) rather than sub-rectangular as in the Alabama *Borealosuchus* though the incomplete preservation of the lacrimal in the Alabama *Borealosuchus* precludes anything but a tentative comparison (McCormack, 2019). The lacrimal foramen is present in the rostral orbit wall, in the medial portion of the lacrimal.

Prefrontal—The caudal portion of the prefrontals is preserved in DMNH EPV.60862 (Fig. 2A, E, I) in addition to the intact prefrontals of DMNH EPV.136252 (Fig. 2C, G, H). The dorsal surface is smooth. The prefrontal forms half of the medial border of the orbit, extends rostrally to between the 5th and 4th alveolus (counted from caudal), and is significantly shorter than the lacrimal. The prefrontal–lacrimal morphology most resembles that of *B. sternbergii* with a lacrimal longer than the prefrontal, whereas the other species of *Borealosuchus* have more elongate prefrontals and lacrimals of the same length (Fig. 7). The prefrontal contacts the nasal rostrally in DMNH EPV.136252 and is nearly linear in its lateral contact with the lacrimal and medial contact with the frontal (Fig. 2C, G, H). The contact with the lacrimal is oriented rostromedially rather than rostrocaudally, similar to the condition noted for the Alabama *Borealosuchus* (McCormack, 2019; Fig. 7). In DMNH EPV.136252, the prefrontal pillar is solid, rostrocaudally broad dorsally, and narrow ventrally. The medial process is ovate, expanded both dorsoventrally and rostrocaudally, with a long rostrocaudal axis.

Frontal—In DMNH EPV.136252, the long, untextured rostral process of the single, co-ossified frontal is broad and U-shaped in its visible contact with the nasals (Fig. 2C, G, H) rather than forming an acute point as in the Alabama *Borealosuchus* and *B. acutidentatus* (McCormack, 2019; Sternberg, 1932) or a narrow, forked process as in *B. griffithi* (Wu et al., 2001; Fig. 7), though it extends a rostral process ventral to the nasals. The frontal is expanded rostrally, and caudally it constricts mediolaterally between the prefrontals (Fig. 2C, G, H). It forms the caudal half of the medial border of the orbits, becoming increasingly textured and expanding caudally to contact the parietal with a convex border. This condition (concavo-convex frontoparietal suture) is, also present in *B. sternbergii* (Gilmore, 1910) distinct from the linear suture present in all other species of *Borealosuchus* (Hester, 2018; McCormack, 2019; Fig. 7). The frontal approaches the supratemporal fenestra, but incomplete preservation in both DMNH EPV.136252 and DMNH EPV.60862 obscures whether the frontal enters the fossa (Fig. 2A, C, E, H, I). The difference in shape between the frontals of DMNH EPV.136252 and DMNH EPV.60862 (bowed further dorsally in the latter) likely reflects a younger ontogenetic stage of DMNH EPV.60862; large orbit and brain volumes relative to skull size result in a broad, rounded frontal in younger crocodylians (Harris, 2015; Mook, 1921; Watanabe et al., 2019). The ventral surface of the frontal exhibits a fossa, the shape of which follows the borders of the frontal and is representative of the dorsal impression of the olfactory tract (Fig. 3A, E, I).

Jugal—Only the portion of the jugal rostral to the ascending process is preserved in DMNH EPV.136252 (Fig. 2C, G, H) and the portion of the jugal just ventral to the ascending process in DMNH EPV.60862 (Fig. 3B). The right jugal is almost complete in DMNH EPV.144434 except for the rostral and caudal most ends (Fig. 6A, B). In lateral view, the jugal is dorsoventrally tall, at its tallest at the caudal most extent of the maxilla. The dorsolateral surface is textured with large round pits (Fig. 2C) and there is a rounded ridge forming the ventrolateral border of the orbit on the dorsolateral surface of the element. There does not appear to be a recess on the rostroventral surface of the jugal, lateral to the maxillary tooth row as described by Wu et al. (2001) and Lindblad et al. (2022) for *B. griffithi* (Fig. 3B). The ascending process is short and the same width its entire extent (Figs. 2C, G, H, 3B, C, G, H). On the medial surface of the jugal, just rostral to the base of the ascending process of the postorbital bar, there is an enlarged fossa, in which the large siphonial foramen (also known as the medial jugal foramen) sits. This has been noted as unique to *B. sternbergii* specimens previously (Brochu, 1997; Gilmore, 1910; Wu et al., 2001) but in fact is present more broadly in *B. formidabilis* as well (mentioned by Erickson, 1976; Wu et al., 2001; personal observation, 2023) and thus recoded for *B. formidabilis* for phylogenetic analysis, see below.

Postorbital—The postorbital is incompletely preserved in both DMNH EPV.136252 and DMNH EPV.60862 (Fig. 2A, C, E, H, I). The descending process forms the dorsal two-thirds of the slender postorbital bar, contacting the ascending process of the jugal caudomedially (Fig. 2C, G, H). The postorbital bar does not bear any prominent processes. The postorbital bar is inset medially from both the jugal and dorsal skull table and angled dorsocaudally (Figs. 2C, G, H, 4A). The postorbital contacts the parietal, squamosal, and quadrate, but the exact nature of these sutures cannot be discerned.

Parietal—The parietal is a singular, solid, co-ossified element, present in DMNH EPV.136252, 60862, and 144434, though damaged caudally in DMNH EPV.136252 (Fig. 2A, C, E, G–I) and obscured rostrally in DMNH EPV.144434 (Fig. 6A, B). In dorsal view, it is rounded and concave in its rostral contact with the frontal and V-shaped in its caudal contact with the supraoccipital (Fig. 2A, C, E, G–I). The deep concavity on the caudal surface resembles the supraoccipital-parietal contact in *B. griffithi* (Wu et al., 2001). The parietal enters the supratemporal fossa, but because of incomplete preservation the extent of the rostrolateral process is unknown (Fig. 2A, E, I). The parietal forms the dorsomedial surface of the temporoorbital canal. Its contact with the laterosphenoid is visible in dorsal view in the rostromedial supratemporal fossa, and the parietal contacts the quadrate in a rostrocaudal suture within the fossa (Fig. 2A, E, I). In DMNH EPV.60862, the parietal contacts the prootic in the caudomedial supratemporal fossa. The parietal is not in contact with the squamosal on the posterior wall of the supratemporal fenestra, being separated by the temporoorbital canal and is only in contact with the squamosal on the caudal skull table in a rostrocaudal, sinuous suture.

Supraoccipital—The supraoccipital is damaged in DMNH EPV.136252 and complete in DMNH EPV.60862 and DMNH EPV.144434, in which it occupies a small portion of the caudal skull table (Figs. 2A, C, E, G–I, 5, 6A, B). The supraoccipital occupies an equal portion of the caudal margin of the skull

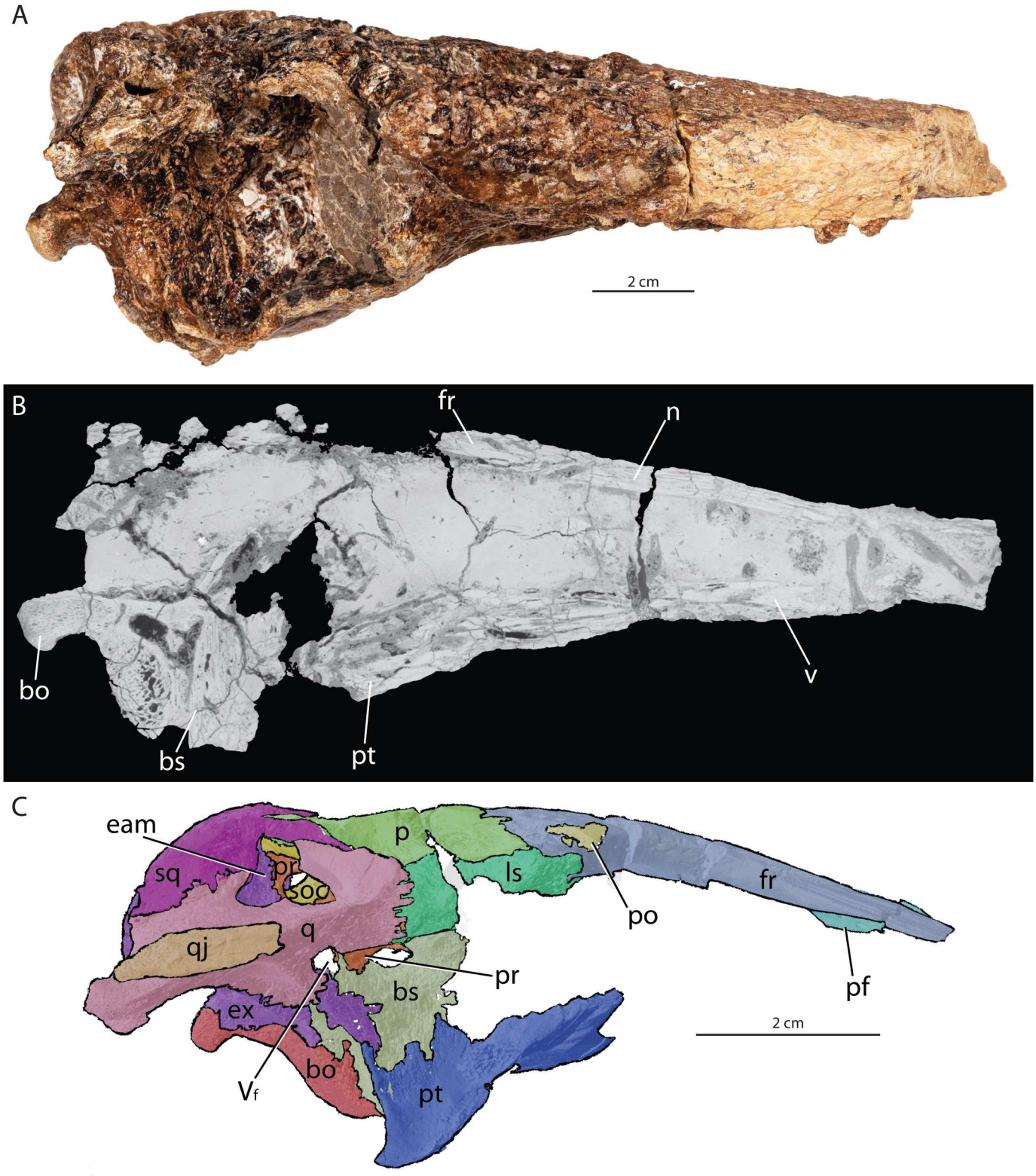

FIGURE 4. *Borealosuchus sternbergii.* **A**, fossil material and **B**, CT slice of DMNH EPV.136252 and CT reconstruction of **C**, DMNH EPV.60862. **A**, right lateral view; **B**, midline sagittal slice showing location of the vomer; **C**, left lateral view (reflected). **Abbreviations**: **bo**, basioccipital; **bs**, basisphenoid; **eam**, external auditory meatus; **ex**, exoccipital; **fr**, frontal; **ls**, laterosphenoid; **n**, nasal; **p**, parietal; **pf**, prefrontal; **po**, postorbital; **pr**, prootic; **pt**, pterygoid; **q**, quadrate; **qj**, quadratojugal; **soc**, supraoccipital; **sq**, squamosal; **v**, vomer; $\mathbf{V_f}$, trigeminal foramen.

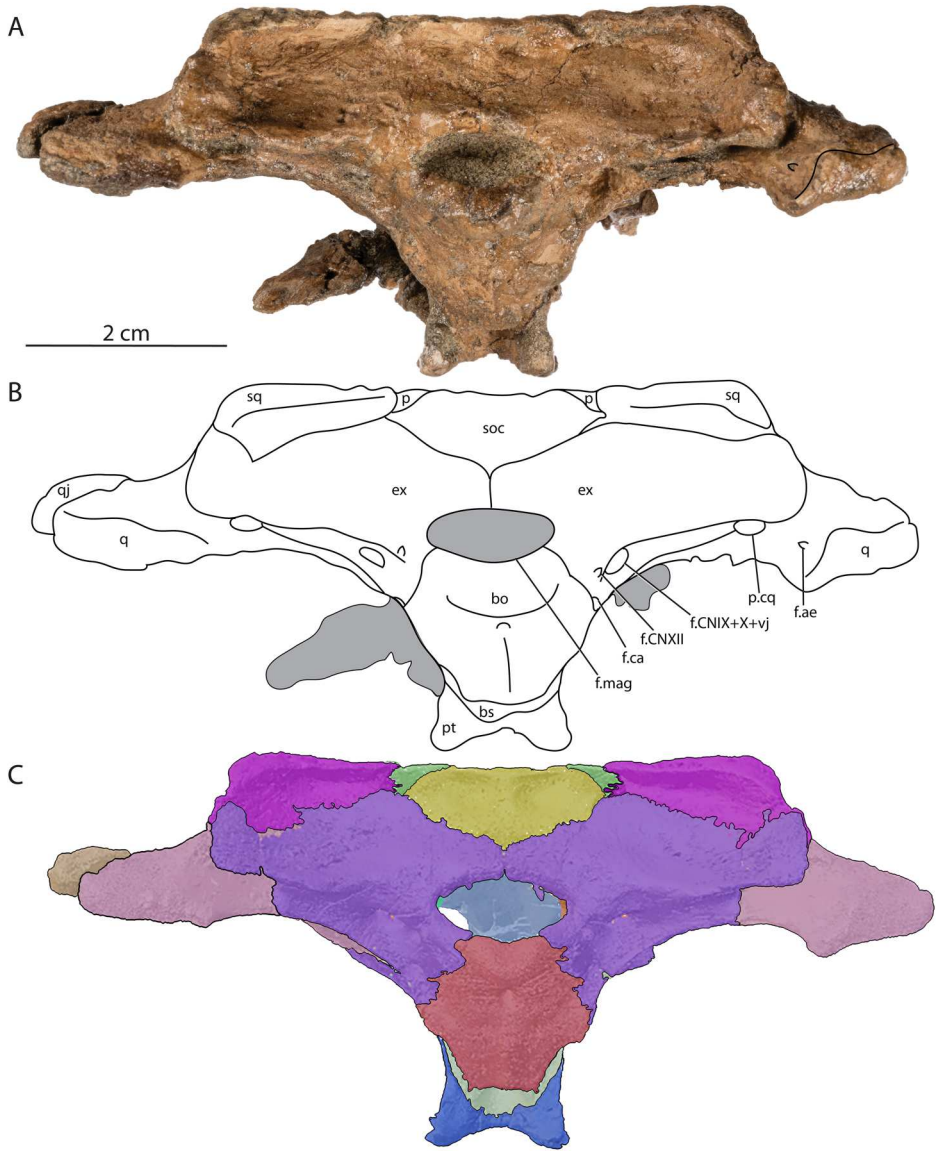

FIGURE 5. Occipital view of *Borealosuchus sternbergii* fossil material (DMNH EPV.60862). **A**, fragmentary cranium; **B**, line drawing; **C**, CT reconstruction. **Abbreviations**: **bo**, basioccipital; **bs**, basisphenoid; **ex**, exoccipital; **f.ae**, foramen aerum; **f.ca**, foramen for the carotid artery; **f.CNIX + X + vj**, foramen for the glossopharyngeal nerve, vagus nerve, and jugular vein; **f.CNXII**, foramen for the hypoglossal nerve; **f.mag**, foramen magnum; **p.cq**, cranioquadrate passage; **p**, parietal; **pt**, pterygoid; **q**, quadrate; **qj**, quadratojugal; **soc**, supraoccipital; **sq**, squamosal.

table as the parietal is similar to the condition in *B. griffithi* (Wu et al., 2001) and unlike other species of *Borealosuchus* in which the supraoccipital occupies a much smaller amount of space (Fig. 7). The supraoccipital contributes a triangular portion of the skull table though in dorsal view, the ventrally deflecting lateral extent is also visible ventral to the caudolateral border of the parietal (Fig. 2A, E, I). In occipital view, the supraoccipital is triangular, tapering ventrally in its contact with the exoccipital and never contacting the squamosal (Fig. 5). Instead, it forms the medial border of the temporoorbital canal. The caudal border of the supraoccipital overhangs the occipital surface, and two shallow fossae are present lateral to a midline ridge.

Squamosal—The single preserved squamosal of DMNH EPV.136252 is quite damaged and those of DMNH EPV.60862 and 144434 are incomplete (Figs. 2A, C, E, G–I, 4C, 5). The squamosal contacts the postorbital rostrally and a rostrolateral process extends to the postorbital bar as in *B. griffithi* (Wu et al., 2001; Fig. 4C). The caudolateral process of the squamosal extends caudal to the edge of the skull table nearly to the caudal most extent of the exoccipital paroccipital process, bearing no features and possessing horizontal sides (Fig. 5). In dorsal view, the squamosal is convex where it overhangs the external auditory meatus rather than concave as seen in the Alabama *Borealosuchus* (McCormack, 2019) or linear as in the other species of *Borealosuchus* (Fig. 2A, E, I, right side is complete). The squamosal comprises the dorsal border and dorsal half of the smooth caudal border of the external auditory meatus where it is in contact with the quadrate. In lateral view, the squamosal is convex dorsally and meets the quadrate in a linear, caudoventrally oriented suture (Fig. 4C). The rims of the squamosal groove are not preserved. The caudal border of the squamosal overhangs the occipital surface creating a concave lateral occipital surface with the exoccipitals (Fig. 5). The squamosal forms the dorsolateral border of the temporoorbital canal.

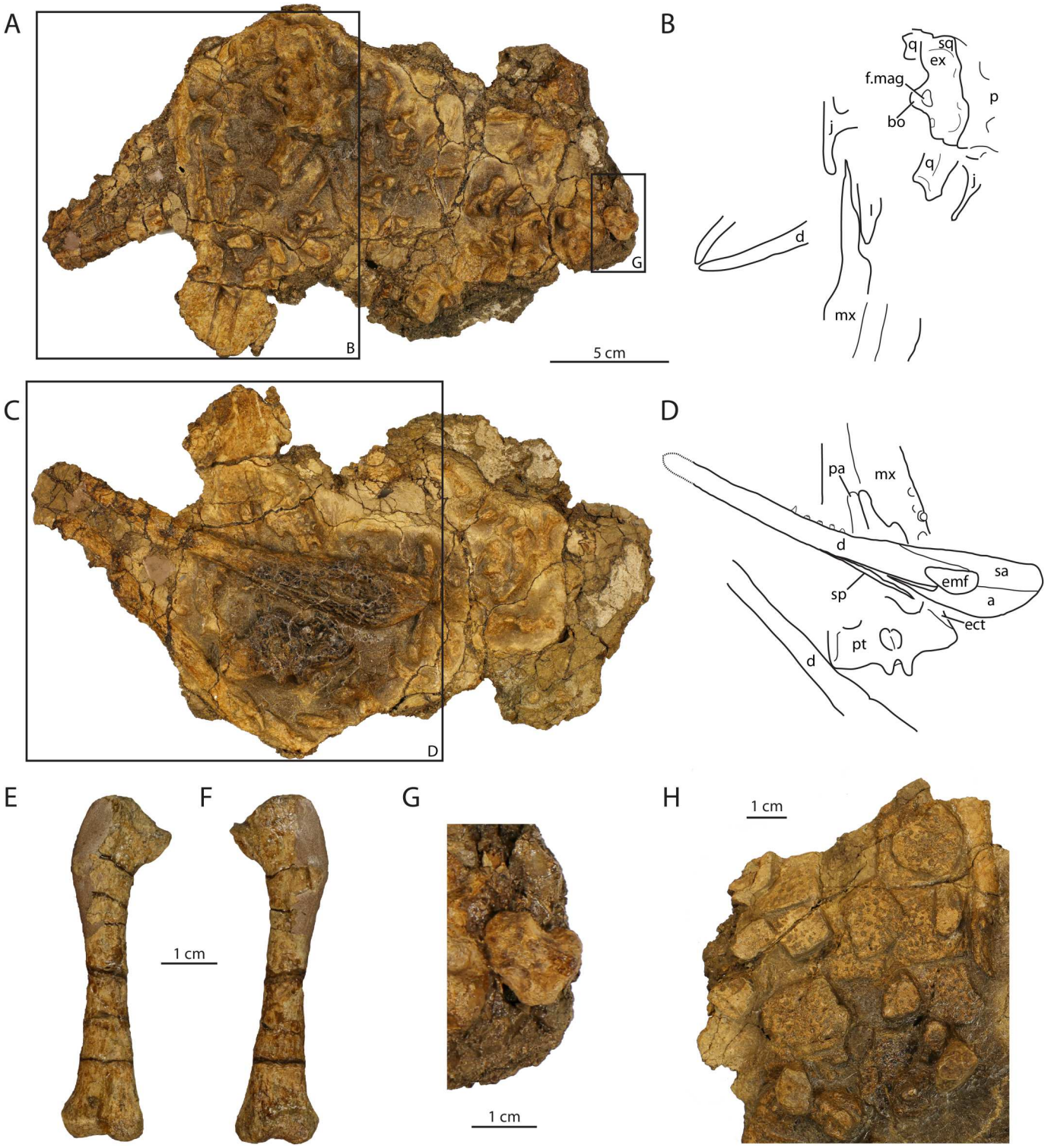

FIGURE 6. Concreted *Borealosuchus sternbergii* fossil material (DMNH EPV.144434). **A**, dorsal view of rostral skull region, medial view of dentaries, and caudal view of occipital region; **B**, line drawing of area indicated in (A); **C**, ventral view of palate, lateral view of left mandible, and ventral view of right mandible; **D**, line drawing of area indicated in (C); **E**, caudal view of incomplete humerus; **F**, rostral view of incomplete humerus; **G**, vertebra, enlarged from area indicated in (A); **H**, osteoderms. **Abbreviations**: **a**, angular; **bo**, basioccipital; **d**, dentary; **ect**, ectopterygoid; **emf**, external mandibular fenestra; **ex**, exoccipital; **f.mag**, foramen magnum; **j**, jugal; **l**, lacrimal; **mx**, maxilla; **p**, parietal; **pa**, palatine; **pt**, pterygoid; **q**, quadrate; **sa**, surangular; **sp**, splenial; **sq**, squamosal.

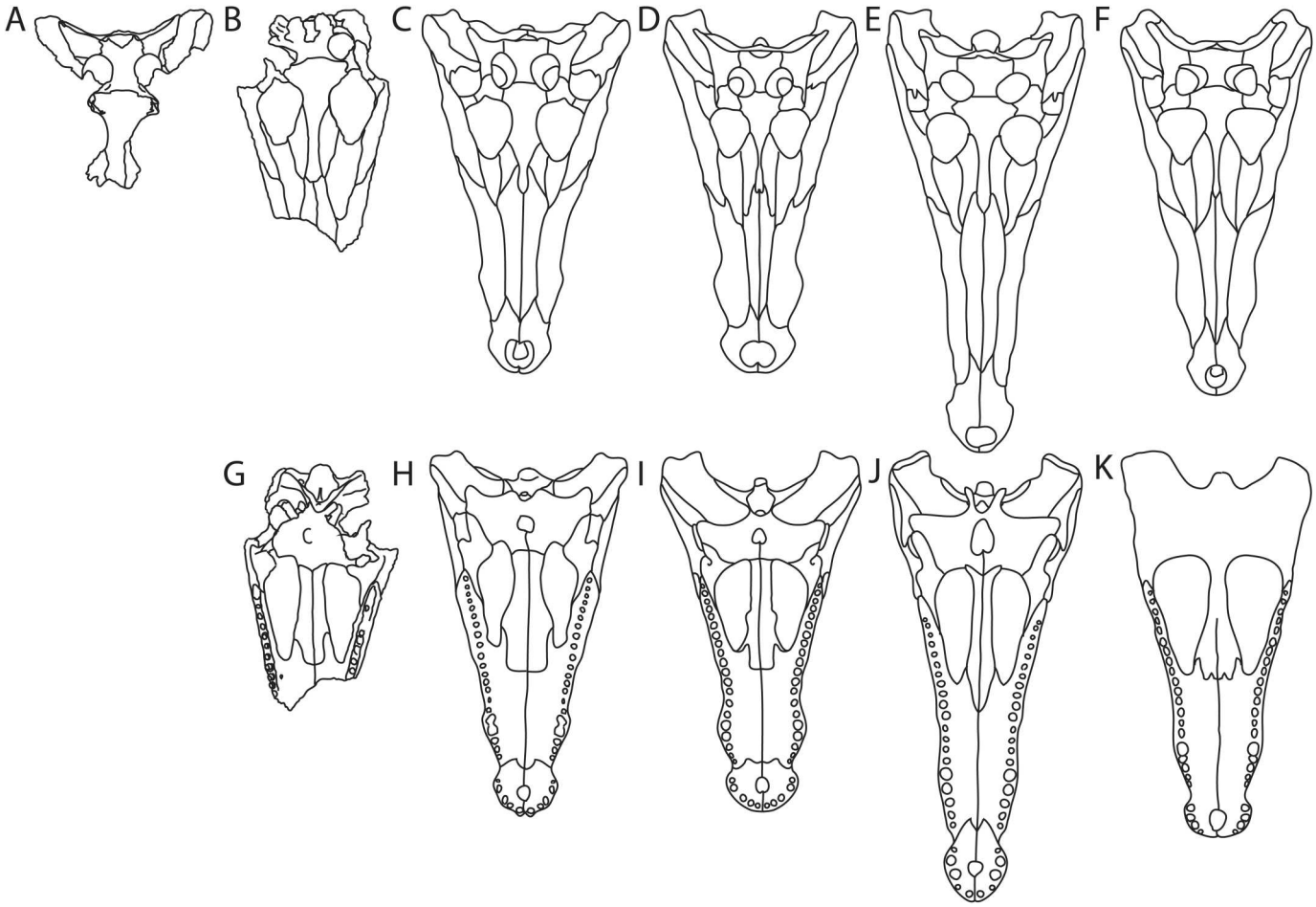

FIGURE 7. General shape and sutural relationships in dorsal view of: **A**, DMNH EPV.60862; **B**, DMNH EPV.136252; **C**, *B. sternbergii*; **D**, *B. griffithi*; **E**, *B. formidabilis*; and **F**, *B. acutidentatus*. Ventral view of **G**, DMNH EPV.136252; **H**, *B. sternbergii*; **I**, *B. griffithi*; **J**, *B. formidabilis*; and **K**, *B. acutidentatus*. Line drawings adapted from Brochu (1997), Sternberg (1932), and Wu et al. (2001).

Palatoquadrate

Maxilla—The maxilla of DMNH EPV.136252 (Fig. 3C, G, H) is only complete to the alveolus 11 (counted from caudal) on the left side and alveolus 9.5 (counted from caudal) on the right side and is likely missing alveoli 8 and 9.5, respectively (Gilmore 1910). Of the 20.5 alveoli present in DMNH EPV.136252, 13 preserve teeth. The alveoli are generally similar in size with a slight decrease in diameter in the final 3–4 alveoli as the maxilla tapers mediolaterally. The two portions of maxillae preserved in DMNH EPV.60862 and that preserved of DMNH EPV.144434 also possess linear, similarly sized alveoli (Figs. 3D, F, 6C, D). The teeth are smooth, similarly sized, and circular in cross section and none of the tips of the crowns are preserved. The preserved portion of the tooth row of DMNH EPV.136252 is nearly linear with a slight lateral curvature (Fig. 3C, G, H). Triangular lingual occlusion pits for dentary teeth are present between the maxillary alveoli beginning rostromedial to the 7th alveolus (counted from caudal). The five preserved occlusion pits on the left side increase in size rostrally. There is a small neurovascular foramen present medial to the 9th maxillary alveolus (counted from caudal) on the left side that may be for the palatine ramus of the trigeminal nerve (Fig. 3C, G, H).

Caudally, the maxilla terminates rostral to the lower temporal bar and tapers mediolaterally between the laterally placed jugal and the medially placed ectopterygoid (Fig. 3C, G, H). The maxilla comprises much of the linear lateral border of the suborbital fenestra, visible in DMNH EPV.136252, 60862, and 144434 (Figs. 3C, D, G, H, 6C, D). The contact with the palatines is broad and occurs on the rostromedial border of the suborbital fenestra (Fig. 3C, G, H).

Ectopterygoid—There is a single ectopterygoid associated with the DMNH EPV.60862 material, however it is not articulated and non-*Borealosuchus* suchians have been identified from the same locality, so its assignment remains uncertain. The ectopterygoid is preserved in DMNH EPV.136252 and 144434 (Figs. 3C, G, H, 6C, D) and is a rostrocaudally broad, mediolaterally thin element, potentially distinguishing it from *B. threeensis* (Brochu et al., 2012). A small, tapering rostral process passes medial to the caudal two alveoli, and the ectopterygoid is close to the maxillary tooth row (Fig. 3C, G, H). The ectopterygoid forms about one third of the caudolateral border of the suborbital fenestra terminating medial to the maxilla. The pterygoid ramus of the ectopterygoid extends a small flange into the fenestra, creating a convex caudolateral border of the suborbital fenestra, also present in *B. sternbergii*. This flange is present on the right side of DMNH EPV.136252 (Fig. 3C, G, H) and incomplete preservation of the left ectopterygoid and those of DMNH EPV.144434 makes it difficult to determine whether it is present on the left side. The caudolateral contact with the jugal is linear

until the ascending process (Fig. 3C, G, H). There, the ectopterygoid possesses a small tapered dorsal process along the medial postorbital bar up to the ventral extent of the postorbital. The ectopterygoid extends caudoventrally along the rostrolateral edge of the pterygoid, and tapers to a point, terminating before the caudal most extent of the pterygoid (Fig. 6C, D).

Palatine—The rostral process of the palatines is broad and U-shaped as in *B. griffithi* and *B. sternbergii* rather than tapering rostrally as in other *Borealosuchus* species (Erickson, 1976; Gilmore, 1910; Lindblad et al., 2022; Wu et al., 2001; Figs. 3C, G, H, 7). The process extends just past the rostral margin of the suborbital fenestra. The medial margin of the suborbital fenestra is slightly concave with some convexity rostrally, where the palatine extends laterally into the fenestra (Fig. 3C, G, H). Caudally, the lateral edges of the palatines are parallel. The palatines terminate caudally in a V-shaped contact with the pterygoids near the caudomedial border of the suborbital fenestrae (Fig. 3C, G, H).

Pterygoid—The pterygoid is incomplete in both DMNH EPV.136252 and DMNH EPV.60862 and its preservation makes distinguishing features difficult to describe in DMNH EPV.144434 (Figs. 3A, C, E, G–I, 4C, 6C, D). It forms the caudomedial border of the suborbital fenestra and completely surrounds the internal choanae (Fig. 3C, G, H). The choanae are oriented slightly rostroventrally as the surface of the caudal portion of the pterygoid is oriented rostroventrally, though distortion of the pterygoids may play a role in this orientation. The pterygoid surface is flush with the choanal margin, the choanal rim smooth, and there is a recessed septum separating the choanae. The lateral contact with the ectopterygoid is sublinear (Fig. 6C, D). Caudally, the tall, caudal pterygoid processes form the rostral border of the median Eustachian foramen and contact the basisphenoid laterally (Fig. 5).

Vomer—The vomer is preserved in DMNH EPV.136252, though it is only visible in CT scan data and not in palatal view (Fig. 4B). It is a small, mediolaterally thin, oval element on the midline. It is present dorsal to the palatine, extending rostral from its contact with the pterygoid at the rostral extent of the descending process of the prefrontal at about the 3rd tooth (counted from caudal). It extends rostrally to between the 6th and 7th teeth (counted from caudal).

Quadrate—The quadrate is incomplete in both DMNH EPV.136252, 60862, and 144434 (Figs. 2–6). It is visible in contact with the parietal, squamosal, and prootic within the caudomedial supratemporal fenestra (Fig. 2A, E, I). The quadrate surrounds most of the external auditory meatus, contacting the squamosal halfway up the dorsocaudal border (Fig. 4C), rather than at the caudoventral corner as in the Alabama *Borealosuchus* (McCormack, 2019), and at the rostrodorsal meatus. In ventral view, the quadrate-exoccipital suture extends rostromedially (Fig. 3A, C, E, G–I). The cranioquadrate passage is present at the caudolateral extent of the suture in ventral view. It opens caudolaterally, bounded by a dorsally extending, rostrocaudally oriented ridge on the quadrate ventrolaterally and the exoccipital dorsomedially (Fig. 5). The ventral surface of the quadrate exhibits a curved ridge following the caudal border, an attachment for the adductor musculature of the jaw apparatus (Fig. 3A, E, I). On the smooth dorsomedial angle of the quadrate ramus, the foramen aerum is present and small, positioned rostrally at the caudal extent of the paroccipital process of the exoccipital (Fig. 5). The medial hemicondyle is small, with an articular surface angled ventromedially. The condyles are distinct, with a sulcus between, and the rounded lateral hemicondyle does not extend as far caudally as the medial (Fig. 5). Though interpretation is difficult in the specimens, the quadrate likely also forms the caudal border of the trigeminal fossa, contributing to the lateral braincase wall (Fig. 4C).

Quadratojugal—The quadratojugal is only preserved as a small piece of bone dorsolateral to the left quadrate of DMNH EPV.60862 and too poorly preserved in DMNH EPV.144434 for further description (Figs. 2–5). The sigmoidal sutural surface is apparent further rostrally but incomplete preservation precludes a more-detailed description.

Braincase

Laterosphenoid—The laterosphenoids of DMNH EPV.60862 and 136252 are minimally preserved and difficult to interpret (Figs. 2, 3, 4C). They form some of the rostral border of the trigeminal fossa, the entire laterosphenoid bridge (visible in CT data), and the rostrolateral braincase wall. Dorsally, the laterosphenoid is in contact with the frontal and parietal and potentially the postorbital, caudally with the prootic (medially) and quadrate (laterally), and ventrally with the basisphenoid (Fig. 2A, C, E, G–I). The laterosphenoid is visible in dorsal view, forming the rostromedial floor of the supratemporal fossa. The capitate process is oriented rostrocaudally.

Prootic—The prootics of DMNH EPV.60862 and 136252 are visible in lateral view ventral to the quadrate and dorsal to the basisphenoid at the caudal border of the trigeminal fossa (Fig. 4C). The prootic contributes to the lateral braincase wall and forms the caudomedial border of the trigeminal fossa. Rostrally it contacts the laterosphenoid (Fig. 4C), dorsally the parietal and potentially the supraoccipital, caudally the exoccipital, laterally the quadrate (Fig. 2A, E, I), and ventrally the basisphenoid. The prootic is three-dimensionally complex; only visible in the CT data are foramina for the facial and vestibulocochlear nerves (cranial nerves VII and VIII, respectively) on its medial surface and the rostral half of the semicircular canals. The prootic is visible in dorsal view, forming a portion of the caudomedial floor of the supratemporal fossa and temporoorbital canal (Fig. 2A, E, I).

Exoccipital—The exoccipital (here including the fused opisthotics) is preserved in DMNH EPV.60862, 136252, and 144434 and makes up much of the caudal surface of the skull and caudolateral surface of the braincase (Fig. 5). Rostrally it contacts the basisphenoid and prootic, ventrally the basioccipital, dorsally the supraoccipital and squamosal, and laterally the quadrate (Figs. 2A, E, I, 3A, E, I, 4C). The dorsal articulation with the supraoccipital is concave and the exoccipital forms the ventral border of the temporoorbital canal (Fig. 5). At its midline, the exoccipitals remain unfused dorsal to the foramen magnum. The exoccipital surrounds the foramen magnum, dorsally and laterally, extending processes ventromedially, terminating dorsolateral to the basioccipital tubera (Fig. 5). The smooth paroccipital process extends laterally, remaining dorsoventrally broad to its lateral extent. The ventral edge of the process is a ridge that overhangs and forms the dorsomedial border of the cranioquadrate passage, as described in *B. formidabilis* (Erickson, 1976; Fig. 5). Ventral to this ridge and dorsal to the ridge-like contact with the quadrate in a mediolaterally oriented depression are the foramina for the glossopharyngeal (cranial nerve [CN] IX), vagus (CN X), and hypoglossal nerves (CN XII; Fig. 4). These nerves exit through numerous foramina located just ventrolateral to the foramen magnum, with the foramina for the hypoglossal nerve located medial to the fossa housing the foramina for the glossopharyngeal and vagus nerves and the jugular vein (Fig. 5). Ventral to these foramina, there is a larger foramen for the passage of the carotid artery. The exoccipital extends a slender process ventral to the foramen for the carotid artery to the broadest portion of the basioccipital.

The exoccipital houses the caudal half of the semicircular canals. On its medial surface, the foramina for the

glossopharyngeal and vagus nerves (CN IX and X, respectively) are present rostrodorsal to the foramina for the hypoglossal nerve (CN XII).

Basisphenoid—Like the laterosphenoid, the basisphenoid of DMNH EPV.60862 and 136252 is incomplete and difficult to interpret (Figs. 3A, C, E, G–I, 4C). The basisphenoid forms the rostral floor of the braincase, contacting the laterosphenoid, quadrate, and prootic dorsally forming a smooth rostral braincase wall, pterygoid and palatine ventrally, and the exoccipital and basioccipital caudally. It appears to form some of the ventral portion of the trigeminal fossa though it is not exposed extensively on the braincase wall rostral to the trigeminal foramen (Fig. 4C). Only visible in the CT data, foramina for the palatine ramus of the facial nerve are present in DMNH EPV.60862 ventrolateral to where the basisphenoid rostrum would extend and the lateral carotid foramen opens lateral to the basisphenoid. The basisphenoid is exposed caudolaterally, as a thin dorsoventrally oriented strip present between the quadrate and the basioccipital (Fig. 5). In occipital view, the basisphenoid is exposed as a broad sheet between the basioccipital dorsally and the pterygoids ventrally. It forms the rostral border of the median and more dorsally located lateral Eustachian openings.

Basioccipital—The basioccipital is preserved in DMNH EPV.60862, 136252, and 144434 (Figs. 3A, C, E, G–I, 5). The basioccipital forms the caudal floor of the braincase, contacting the basisphenoid and palatine rostrally and the exoccipital dorsally (Fig. 5). It forms the ventral border of the foramen magnum and caudal border of the median and lateral Eustachian openings. The ovate occipital condyle extends caudally with a concave ventral margin. Ventral to the occipital condyle, the basioccipital extends ventrally, flaring laterally and then narrowing and presenting a dorsoventrally trending ridge along its midline (Fig. 5). This ventral surface faces posteriorly, though the angle is more similar to *B. sternbergii* (Gilmore, 1910) than the posteriorly facing surface in the Alabama *Borealosuchus* (McCormack, 2019).

Mandible

Lower jaws are only preserved in DMNH EPV.144434 and these are fragmentary, with preparation and preservation revealing only left and right dentaries and partial splenials and angulars, and a left partial surangular (largely obscured in medial view; Fig. 6C, D). The mandible has linear margins and possesses an ovate external mandibular fenestra with a rostroventrally oriented axis that tapers rostrally and is rounded caudally.

Dentary—Only visible in dorsal and lateral views, the dentary is elongate and linear in both (Fig. 6A–D). It is dorsoventrally short, only tapering slightly from the caudal most alveolus to its rostral extent. The left dentary preserves at least 12 similarly sized alveoli but likely contained at least 19, the exact number is unknown because of poor preservation. Most teeth are missing the tips of their crowns and are circular in cross section, with one complete, smooth conical tooth that tapers to a point. In lateral view, the posterior portion of the dentary expands dorsoventrally to form much of the rostral border of the external mandibular fenestra (Fig. 6C, D). The dorsal posterior process forms two-thirds of the dorsal border, articulating with the surangular rostral to the caudodorsal corner of the external mandibular fenestra. The ventral process forms one-third of the ventral border, articulating with the angular (Fig. 6C, D).

Splenial—The caudal portion of the splenial is visible in lateral view, having disarticulated and been displaced ventrally (Fig. 6C, D). It extends caudally to the rostral border of the external mandibular fenestra, where it would have contacted the dentary and angular.

Angular—The angular forms the rounded caudoventral edge of the mandible in lateral view (Fig. 6C, D). The ventral rostral process forms the caudal border of the external mandibular fenestra and tapers to a point between the dentary and displaced splenial at the level of the caudal most alveolus. The dorsal rostral process also tapers rostrally, forming the caudoventral border of the external mandibular fenestra (Fig. 6C, D). The angular articulates with the surangular halfway up the caudal border of the external mandibular fenestra in a caudodorsally oriented, linear suture. The retroarticular process is not preserved.

Surangular—The surangular forms the caudodorsal portion of the mandible in lateral view (Fig. 6C, D). It possesses a tapering rostral process that articulates with the dorsal caudal process of the dentary and extends to the caudal most extent of the tooth row. Caudal to the external mandibular fenestra, the dorsal edge of the surangular swells laterally (Fig. 6C, D). No articulation with the articular is visible.

Postcrania and Other Material

Only DMNH EPV.144434 possesses an incomplete left humerus and vertebra and several osteoderms (Fig. 6E–H). The proximal end of the humerus deflects sharply toward where the articular surface would be, however it is broken proximally and missing the articular surface and deltopectoral crest (Fig. 6E, F). The straight shaft narrows distally and then expands towards the distal condyles. The medial and lateral condyle extend distally to the same extent, expanding medially and laterally. They are separated by a shallow depression on the caudal and distal surface and are separated from the shaft on the rostral surface by a mediolaterally oriented ridge. In ventral view, the condyles are angled rostrolaterally. The vertebra is procoelus and has a rostrocaudally oriented keel on the ventral surface of the centrum indicating it is a cervical vertebra (Fig. 6G). The osteoderms are dorsoventrally thin, possess no keel, and have broad, shallow ridges between randomly arranged pitting as seen in other species of *Borealosuchus* (e.g., Erickson, 1976; Lindblad et al., 2022; McCormack, 2019; Wu et al., 2001; Fig. 6H). It is difficult to discern whether a smooth rostral margin is present. The osteoderms are subrectangular and there may be several with rostromedial processes similar to that of other species of *Borealosuchus* (Brochu et al., 2012; Lindblad et al., 2022; McCormack, 2019).

There are also postcranial elements (largely osteoderms) from the Colorado Bluffs study area that likely belong to *Borealosuchus sternbergii* (in DMNH and UCM collections, Figs. S1–S3). The osteoderms (Fig. S1B–F) are similar to those described above although larger. A maxilla fragment (Fig. S2G–H) has a flat dorsal surface in lateral view, a lateral swelling at what is likely the 4th and 5th maxillary alveoli, and a rostral upturn at what is likely the 2nd and 3rd maxillary alveoli, resembling that of other species of *Borealosuchus* (e.g., Gilmore, 1910; Lindblad et al., 2022; Wu et al., 2001). A poorly preserved, partial cranium (Fig. S2) possesses a flat dorsal maxillary surface in lateral view as well, orbits that taper rostrally, elongate suborbital fenestrae, and a palatine with parallel margins as in the *Borealosuchus sternbergii* material described above.

Material (largely osteoderms and fragmentary cranial material) is known from West Bijou, a locality spanning the K–Pg boundary about 45 miles to the northeast of the Corral Bluffs study area (in DMNH and UCM collections, Fig. S1). The osteoderms (Figs. S1A, S3B, D, E) and a maxillary fragment (Fig. S3A) are as described above and a frontal fragment with shallow pitting (Fig. S3C) is known from the same site as the maxilla fragment and some osteoderms. Fragmentary cranial material has been described from the Alexander Site in Littleton, Colorado (Middleton, 1983; Fig. 1). None of this isolated,

fragmentary material allows for identification beyond *Borealosuchus* sp., but given the material was found in the same sediments as the crania referred to *B. sternbergii*, we herein tentatively refer this material to the same taxon.

PHYLOGENETIC RELATIONSHIPS

Phylogenetic Results

Analysis of the individual DMNH specimens recovered the identical topology, placing all three specimens into an unresolved trichotomy in a strict consensus tree from 511 most parsimonious trees (MPTs) with a tree score of 27.50606 (consistency index, CI = 0.30; retention index, RI = 0.77; see Supplementary Material). The combined analysis produced 473 most parsimonious trees (MPTs) with a tree score of 27.46195. We condensed those MPTs into a strict consensus tree (Fig. 8).

High Bremer supports (0.04, low with respect to other results yielded from the Brochu matrix) indicate that the placement of the *Borealosuchus* species complex is less robustly supported with respect to allodaposuchids and the clade comprising Brevirostres (last common ancestor of *Alligator mississippiensis* and *Crocodylus niloticus* and all its descendents; Brochu, 2003) and Planocraniidae than other relationships reflected in the phylogeny. The DMNH specimens are found in a polytomy with *B. sternbergii* and a clade including the rest of the species of *Borealosuchus* in the strict consensus tree (Fig. 8). In other studies, *B. sternbergii* is not always found in a monophyletic clade with other species of *Borealosuchus* (e.g., Cossette & Brochu, 2020; Delfino & Smith, 2012). Here, further *Borealosuchus* sp. placement reflects previous observations by some authors (e.g., Brochu et al., 2012; Delfino et al., 2005; Hastings et al., 2016; McCormack, 2019).

We find *Borealosuchus* defined by the following synapomorphies: atlantal ribs with modest dorsal process on dorsal margin (character 6[0]), an anterior half of the axis neural spine that slopes anteriorly (character 11[1]), very long and slender limb bones (character 36[1]; autapomorphy), a fourth dentary alveolus that is larger than the third and with separated alveoli (character 47[0]), coronoid with rostrally sloping superior edge (character 56[0]), nasals excluded externally from the naris with the nasals and premaxillae still in contact (character 82 [2]), occlusion pits between 7th and 8th maxillary teeth with all other dentary teeth occluding lingually (character 92[1]), a maxillary toothrow that curves laterally broadly posterior to the first six maxillary alveoli (character 94[1]), and a large medial jugal foramen (character 102[1]). Whereas we are unable to assess characters 6, 11, 36, 47, 56, 82, or 94, DMNH EPV.60862 and DMNH EPV.136252 possess large medial jugal foramina and DMNH EPV.136252 does possess some occlusion pits.

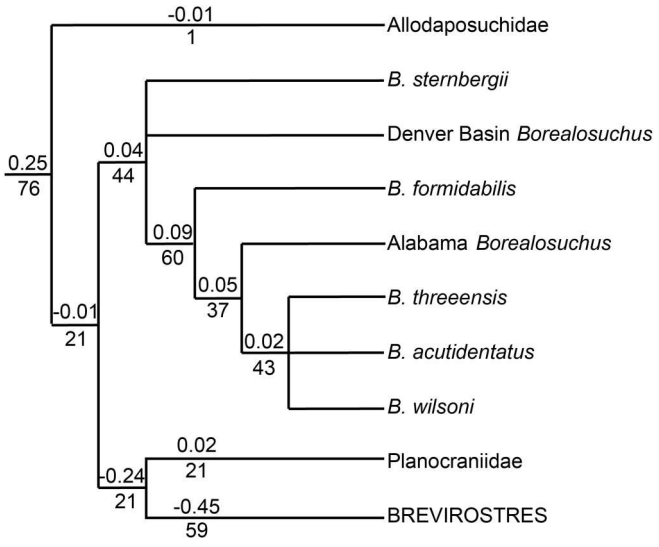

FIGURE 8. Strict consensus tree showing the recovered phylogenetic placement of *Borealosuchus sternbergii* specimens relative to other known *Borealosuchus*. Numbers above node represent combined Bremer support values and numbers below node represent Bootstrap values from 2000 repetitions. We list Bootstrap for all *Borealosuchus*; outside the *Borealosuchus* species complex, the cutoff is 50%.

Borealosuchus sternbergii exclusive of DMNH EPV.60862, DMNH EPV.136252, and DMNH EPV.144434 is supported by a surangular with a spur that borders the dentary toothrow (character 62[0]) and lateral edges of palatines with a lateral process projecting from the palatines into the suborbital fenestra (character 117[1]). We cannot assess characters 62 or 117 in DMNH EPV.60862 or 144434. However in DMNH EPV.136252, the palatines broaden near their rostral contact with the maxillae but preservation obscures whether a distinct ear-shaped process is present as in *Leidyosuchus canadensis* (Wu et al., 2001), *B. griffithi* (Lindblad et al., 2022). In *B. sternbergii* (USNM 6533) this region is asymmetric with the left palatine displaying a shelf-like process not as distinct as *L. canadensis* or *B. griffithi*, and the feature is absent on the other side. Scoring this character with ambiguity indicates that no concrete characters separate DMNH EPV.60862, DMNH EPV.136252, or DMNH EPV.144434 from *B. sternbergii* and therefore we refer these specimens to *B. sternbergii*.

Characters do differentiate *B. sternbergii*, DMNH EPV.60862, DMNH EPV.136252, and DMNH EPV.144434 from the remaining *Borealosuchus* species. Namely, both DMNH EPV.60862, DMNH EPV.136252, and *B. sternbergii* possess concavo-convex frontoparietal sutures between the supratemporal fenestrae (character 151[0]) whereas this suture is linear in *B. formidabilis*, the Alabama *Borealosuchus*, *B. acutidentatus*, *B. wilsoni*, and *B. threeensis*. Additionally, as evident in DMNH EPV.136252 and *B. sternbergii*, the palatine process is broad rostrally (character 116[0]) rather than a thin wedge, the pterygoid ramus of the ectopterygoid is not straight (character 119[1]), and the lacrimal is longer than the prefrontal (character 130[0]) rather than both being elongate and of the same length.

DMNH EPV.60862 and 144434 are not defined by any apomorphies but DMNH EPV.136252 is scored as distinct in the lack of rostral extent of its palatine process (character 115[1]). When examining the rostral extent of the palatine process in *B. sternbergii* (scored as having a palatine process extending significantly beyond the suborbital fenestra), there is asymmetry in *B. sternbergii* (USNM 6533, USNM 5898, Gilmore, 1910) in that the left rostral palatine process and right suborbital fenestra extend further rostrally than the right and left, respectively. The palatal morphology of the right halves of these skulls is comparable to that of DMNH EPV.136252 and therefore this character is not enough to distinguish DMNH EPV.136252 from *B. sternbergii* further supporting the referral. When combined, the Denver Basin taxa are distinguished by rostroventrally oriented choanae (character 122[1]). However, this scoring is tentative because of the juvenile state and incompleteness of the specimens.

Though *B. griffithi* has never been included in a matrix and was not scored for this study, we find a number of features that differentiate it from the DMNH specimens. Particularly, *B. griffithi* has a deep elongated recess of the jugal's anteroventral surface, a maxillary process extending between the jugal and lacrimal, large pits on the parietal, and lateral margin of the palatine with an ear-like process, none of which are present in DMNH EPV. 60862 and 136252 (Lindblad et al., 2022; Wu et al., 2001).

We find no characters distinguishing *Borealosuchus formidabilis* from the remaining species of *Borealosuchus* (Alabama *Borealosuchus*, *B. acutidentatus*, *B. threeensis*, and *B. wilsoni*). Three

characters not preserved or observable in DMNH EPV.60862 and 135252 define the clade including the Alabama *Borealosuchus*, *B. acutidentatus*, *B. threeensis*, and *B. wilsoni*: sutured, paired ventral osteoderms (character 42[2]), a dentary symphysis that extends to the fourth or fifth alveolus (character 49[0]), and an external mandibular fenestra that is present as a narrow slit with no discrete fenestral concavity on the dorsal margin of the angular (character 63[1]). The DMNH specimens are distinct from the Alabama *Borealosuchus* in that it has a squamosal-quadrate suture that extends only to the posteroventral corner of the external auditory meatus (character 148[1]), whereas this suture extends further dorsally in the DMNH specimens. An additional two characters not observed in the DMNH specimens define the Alabama *Borealosuchus*: Round dorsal margin of the iliac blade with a modest dorsal indentation (character 34[1]) and a truncated surangular that does not continue dorsally to the glenoid fossa (character 67[1]). The DMNH specimens are distinct from the clade containing *B. threeensis*, *B. acutidentatus*, and *B. wilsoni* in that the postorbital and parietal are in broad contact (character 150[1]) and in a character not observed in the DMNH specimens; the splenial is excluded from the mandibular symphysis (character 54[1]). Within this clade, we find no characters distinguishing *B. acutidentatus. B. wilsoni* is distinguished by a lingual foramen that perforates the surangular/angular suture (character 69[1]). *B. threeensis* is distinguished by a surangular-dentary suture intersecting the posterodorsal corner of the external mandibular fenestra (character 64[1]) rather than intersecting rostral to the posterodorsal corner as observed in DMNH EPV.144434.

DISCUSSION

Ontogeny

DMNH EPV.60862 is estimated to have a total length of 127.12 cm and DMNH EPV.136252 is estimated to have a total length of 155.98 cm (Table 1). Total lengths from 3–5 meters have been hypothesized for species of *Borealosuchus* (Farlow et al., 2005; Iijima & Kubo, 2020), and Lindblad et al. (2022) identified a specimen of *Borealosuchus* with open neurocentral sutures (indicative of immaturity [Brochu, 1996]) of approximately 2 m. Therefore, it is reasonable to assume immaturity for the DMNH specimens.

Additional features indicate a sub-adult state including the barely prominent ridge on the ventral surface of the quadrate of DMNH EPV.60862 (McCormack, 2019). This ridge is an attachment for the jaw adductor musculature and is prominent in more ontogenetically mature individuals such as the Alabama *Borealosuchus* (McCormack, 2019). The rectangular skull table has also been identified as a feature of small crocodylian specimens (Cossette et al., 2022). Mook (1921) identified several characteristics in crocodylians that are ontogenetically variable, two of which are represented in their sub-adult states in the DMNH specimens. These include: the center of the supratemporal fenestra located lateral to the medial border of the orbit (supratemporal fenestrae migrating medially through ontogeny), and relatively large orbits compared with other *Borealosuchus* specimens (orbit relative size decreasing through ontogeny; Mook, 1921). The bowed frontal noted above in DMNH EPV.60862 is another likely ontogenetic feature reflecting the relatively large eye and brain in young individuals (Harris, 2015; Mook, 1921; Watanabe et al., 2019). Erickson (1976) also noted several ontogenetically variable features upon observation of numerous *B. formidabilis* specimens that are also present in their sub-adult states in the DMNH specimens. These include delicate sculpturing of cranial elements (De Buffrénil et al., 2015), alveoli present in a groove (not distinct), and the placement of the choanae close to the suborbital fenestrae.

Immature ontogenetic status may play a role in ambiguous phylogenetic placement. A tendency of immature individuals to be recovered on the stem of their clade has been documented (Campione et al., 2013; Tsuihiji et al., 2011). For this reason, no new species is erected for the DMNH specimens as they likely represent a sub-adult of *B. sternbergii*. Alternatively, their basal placement by this study with respect to other species of *Borealosuchus* may be an artificial representation of phylogenetic placement.

Biogeographic and Temporal Implications

These specimens expand the geographic range of the *Borealosuchus* species complex into central Colorado, the next closest being *B. wilsoni* from southern Wyoming and northern Colorado (Hester, 2018) and *B.* sp. from Texas (Brochu, 2000; Fig. 10). There are purported *B. acutidentatus* and *B. wilsoni* from the late Paleocene and early Eocene of New Mexico (Cope, 1875; Lucas, 1988; Lucas & Sullivan, 1986) but these identifications are not analyzed (Brochu, 1997). Our new finds fill a spatial gap in southern North America during the Paleocene, where species of *Borealosuchus* are only known from Canada, North Dakota, and Texas (Fig. 10). Temporally, the holotype of *B. sternbergii* is from the latest Cretaceous (Maastrichtian), and other material from the lower Paleocene Tullock Formation of Montana and Ludlow Formation of North Dakota has tentatively been referred to *B. sternbergii* (Brochu, 1997). Our finds definitively expand this range for *B. sternbergii* across the K–Pg boundary into the early Paleocene. Importantly, *B. sternbergii*, along with the soft-shell turtle *Axestemys infernalis* (Joyce et al., 2019), represent the two largest vertebrates from North America that survive the end-Cretaceous mass extinction.

The trans-quadratic skull proxy for body size (O'Brien et al., 2019) suggest *B. sternbergii* specimens up to ~230 cm and body mass of ~55 kg (UCMP 173976; Table 1). Large body size is generally selected against across the K–Pg boundary, exemplified by the extinction of all non-avian dinosaurs (MacLeod et al., 1997), as well as large birds (Field et al., 2018), mammals (Wilson, 2013), and anurans (Feijó, et al., 2023). *B. sternbergii* and *A. infernalis* both run counter to this trend and their inferred generalist diet, slow metabolism, and inhabitation of aquatic environments likely helped these taxa persist across the K–Pg boundary (Buffetaut, 1990; Robertson et al., 2004).

Of other *Borealosuchus* species, only the Alabama *Borealosuchus* is known from the Late Cretaceous (Campanian). *B. threeensis* is found in a deposit hypothesized to represent the K–Pg boundary (Obasi et al., 2011; Voegele et al., 2021), whereas *B. griffithi* is known from the early Paleocene, *B. acutidentatus* and *B. formidabilis* from the middle Paleocene, and *B. wilsoni* from the early Eocene (Figs. 9, 10). The western Maastrichtian and early Paleocene occurrence of *B. sternbergii*, the most basal member of *Borealosuchus*, eastern K–Pg occurrence of *B. threeensis*, and eastern Campanian appearance of the Alabama *Borealosuchus* mean that the pattern of dispersal of the clade remains mysterious as earliest records are from both sides of the Western interior Seaway (McCormack, 2019; Williams et al., 2018) and post- K–Pg occurrences of species of *Borealosuchus* are widespread.

Eusuchians co-occurring in the Denver Basin during the early Paleocene include a *Navajosuchus*-like, blunt-snouted, globe-toothed alligatorine (Lyson et al., 2019) indicating occupation of separate niches. The relatively longirostrine members of the *Borealosuchus* species complex are expected to have occupied a generalist niche, with a potential specialization for piscivory based on its elongate rostrum, dentition, and orbit placement (Erickson, 1976; Stout, 2012). The piscivorous niche has also been hypothesized for champsosaurs (Erickson, 1972) which have also been recorded from the region (Middleton, 1983),

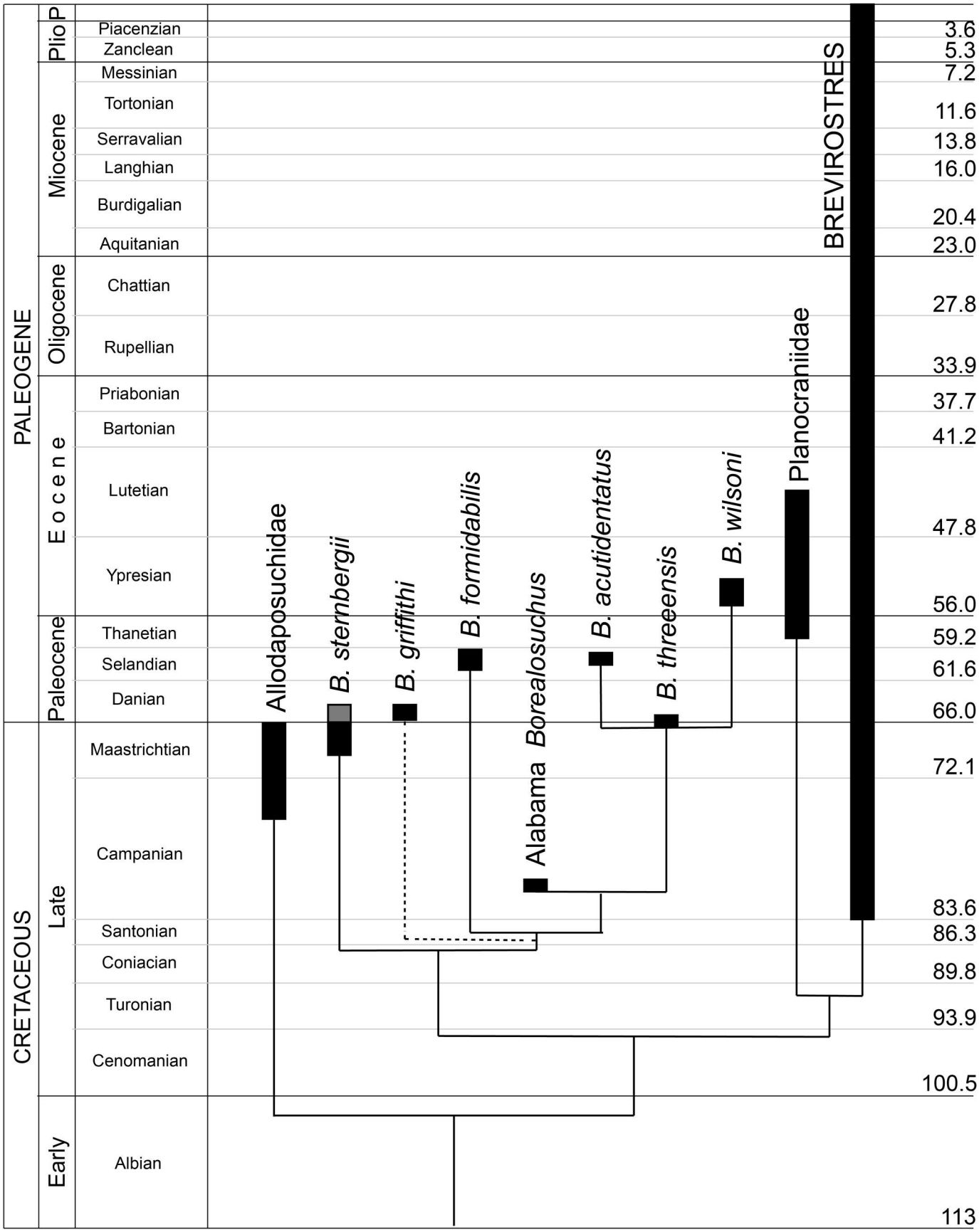

FIGURE 9. Time-calibrated phylogeny including new *Borealosuchus sternbergii* specimens as a transparent box, extending the previous known range. Dotted line for *B. griffithi* represents tentative phylogenetic placement (Wu et al., 2001).

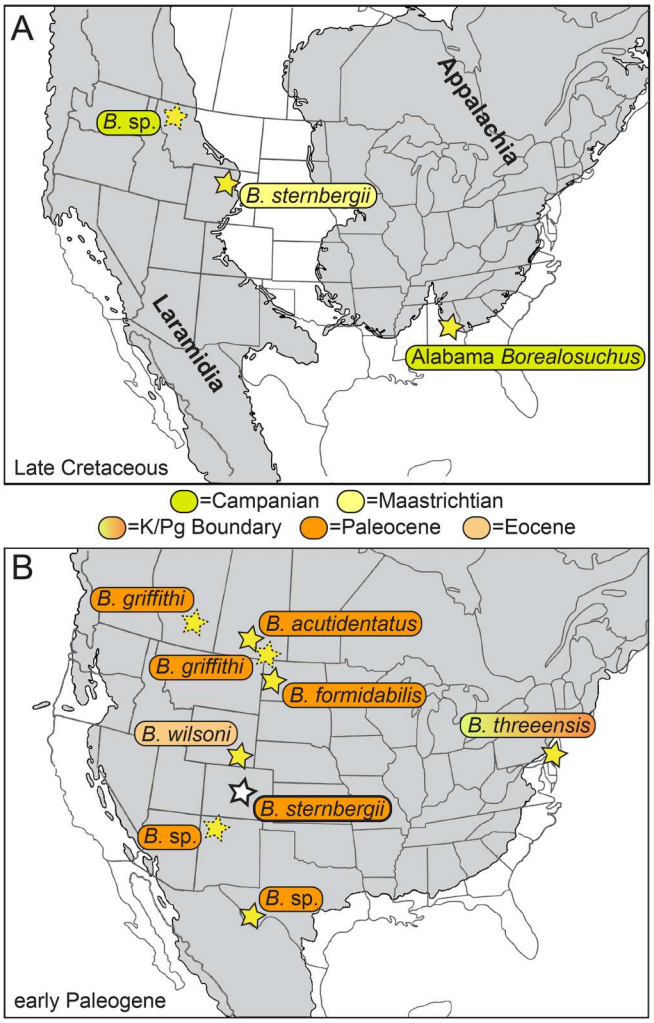

FIGURE 10. Paleobiogeographic distribution of *Borealosuchus*. **A**, Late Cretaceous; **B**, early Paleogene. Bolded star represents newly referred material. Dotted stars represent specimens not placed phylogenetically. Modified from Blakey (North American Key Time Slices ©2013 Colorado Plateau Geosystems Inc.) and McCormack (2019).

although are rare compared with the two eusuchian taxa (Lyson et al., 2019). Limb proportions have been hypothesized to indicate terrestrial specialization in species of *Borealosuchus* (Erickson, 1976). However, comparative data reveal limb proportions are more complicated and hypothesizing locomotor strategy is more complex; members of the *Borealosuchus* species complex have similar hindlimb ratios to crocodyloids, similar forelimb ratios to alligatoroids, and an average stylopodial length (Iijima et al., 2018), perhaps indicating the ancestral condition for Crocodylia.

CONCLUSIONS

These specimens extend the record of *B. sternbergii* across the K–Pg boundary, adding a record of eusuchian extinction survivorship. In addition to a temporal expansion, these specimens expand the geographic range of the *Borealosuchus* species complex into Colorado and contribute to a better understanding of the ontogeny of *B. sternbergii*, as the most immature specimens documented. Overall, they fill an important gap in the fossil record of the *Borealosuchus* species complex and help constrain biogeographic dispersal patterns for the clade. Analysis of *B. griffithi* and discovery and identification of more members of *Borealosuchus* from eastern deposits are the logical next steps in clarifying phylogenetic relationships and dispersal of species of *Borealosuchus*.

ACKNOWLEDGMENTS

We thank K. Weissenburger for finding DMNH EPV.60862 and for stratigraphic data. We also thank J. Englehorn, N. Toth, K. Carpenter, S. Bastien, S, Begin, and S. Rush for preparation of specimens, K. Mackenzie and J. Van Veldhuizen for access to collections, R. Wicker for photography, the University of Texas High-Resolution X-ray Computed Tomography Facility and M. Colbert, J. Maisano, and D. Edey for CT scanning the material, G. Morlock for segmentation, and the Denver Museum of Nature & Science Digital Research Laboratory (L. Dougan, F. Duffy, and E. Panigot) for assistance and discussion. Norwood Properties, City of Colorado Springs, Waste Management, J. Hilaire, D. Lumb, J. Carner, and Aztec Family Raceway provided access to their property. Funding was provided by Lyda Hill Philanthropies, the National Geographic Society (NGS-93605R-22), the David B. Jones Foundation, M.L. and S.R. Kneller, and the National Science Foundation (NSF-FRES-231766) to TRL. The conclusions presented here are those of the authors and do not represent the views of the United States Government.

AUTHOR CONTRIBUTIONS

TRL and EJL designed the study. EJL segmented CT data and exported 3D mesh models. TRL (Fig. 1) and EJL (Figs. 2–10) assembled figures. EJL and HP assembled character matrix. HP conducted phylogenetic analyses. EJL prepared and edited the manuscript. HP and TRL edited the manuscript.

DATA AVAILABILITY STATEMENT

The authors confirm that the data supporting the findings of this study are available within the article and its supplementary materials, Morphosource, Project ID: 000581588.

DISCLOSURE STATEMENT

No potential conflict of interest was reported by the author(s).

ORCID

Emily J. Lessner http://orcid.org/0000-0003-0774-1613

SUPPLEMENTARY FILES

Supplementary File 1.docx: Figs. S1–S3
Supplementary File 2.docx: Character list and scorings for DMNH EPV.60862, 136252, and 144434
Supplementary File 3.nex: Matrix and Tree Files

LITERATURE CITED

Barclay, R. S., Johnson, K. R., Betterton, W. J., & Dilcher, D. L. (2003). Stratigraphy and megaflora of a KT boundary section in the eastern Denver Basin, Colorado. *Rocky Mountain Geology*, *38*(1), 45–71. doi:10.2113/gsrocky.38.1.45

Beardmore, S. R., Orr, P. J., Manzocchi, T., Furrer, H., & Johnson, C. (2012). Death, decay and disarticulation: modelling the skeletal taphonomy of marine reptiles demonstrated using Serpianosaurus

(Reptilia; Sauropterygia). *Palaeogeography, Palaeoclimatology, Palaeoecology*, *337*, 1–13. doi:10.1016/j.palaeo.2012.03.018

Benton, M. J., & Clark, J. M. (1988). Archosaur phylogeny and the relationships of the Crocodylia. *The phylogeny and classification of the tetrapods*, *1*, 295–338.

Bertrand, O. C., Shelley, S. L., Williamson, T. E., Wible, J. R., Chester, S. G., Flynn, J. J., … Brusatte, S. L. (2022). Brawn before brains in placental mammals after the end-Cretaceous extinction. *Science*, *376* (6588), 80–85. doi:10.1126/science.abl5584

Brochu, C. A. (1996). Closure of neurocentral sutures during crocodilian ontogeny: implications for maturity assessment in fossil archosaurs. *Journal of Vertebrate Paleontology*, *16*(1), 49–62. doi:10.1080/02724634.1996.10011283

Brochu, C. A. (1997). A review of "*Leidyosuchus*"(Crocodyliformes, Eusuchia) from the Cretaceous through Eocene of North America. *Journal of Vertebrate Paleontology*, *17*(4), 679–697. doi:10.1080/02724634.1997.10011017

Brochu, C. A. (1999). Phylogenetics, taxonomy, and historical biogeography of Alligatoroidea. *Journal of Vertebrate Paleontology*, *19*(S2), 9–100. doi:10.1080/02724634.1999.10011201

Brochu, C. A. (2000). *Borealosuchus* (Crocodylia) from the Paleocene of big bend national park, Texas. *Journal of Paleontology*, *74*(1), 181–187. doi:10.1666/0022-3360(2000)074<0181:BCftpO>2.0.CO;2

Brochu, C. A. (2003). Phylogenetic approaches toward crocodilian history. *Annual Review of Earth and Planetary Sciences*, *31*(1), 357–397. doi:10.1146/annurev.earth.31.100901.141308

Brochu, C. A. (2004). A new Late Cretaceous gavialoid crocodylian from eastern North America and the phylogenetic relationships of thoracosaurs. *Journal of Vertebrate Paleontology*, *24*(3), 610–633. doi:10.1671/0272-4634(2004)024[0610:ANLCGC]2.0.CO;2

Brochu, C. A. (2012). Phylogenetic relationships of Palaeogene ziphodont eusuchians and the status of *Pristichampsus* Gervais, 1853. *Earth and Environmental Science Transactions of the Royal Society of Edinburgh*, *103*(3-4), 521–550. doi:10.1017/S1755691013000200

Brochu, C. A., Parris, D. C., Grandstaff, B. S., DentonJrR. K., & Gallagher, W. B. (2012). A new species of *Borealosuchus* (Crocodyliformes, Eusuchia) from the Late Cretaceous–early Paleogene of New Jersey. *Journal of Vertebrate Paleontology*, *32* (1), 105–116. doi:10.1080/02724634.2012.633585

Buffetaut, E. (1990). Vertebrate extinctions and survival across the Cretaceous-Tertiary boundary. *Tectonophysics*, *171*(1-4), 337–345. doi:10.1016/0040-1951(90)90108-K

Buscalioni, A. D., Piras, P., Vullo, R., Signore, M., & Barbera, C. (2011). Early eusuchia crocodylomorpha from the vertebrate-rich Plattenkalk of Pietraroia (Lower Albian, southern Apennines, Italy). *Zoological Journal of the Linnean Society*, *163*(suppl_1), S199–S227. doi:10.1111/j.1096-3642.2011.00718.x

Campione, N. E., Brink, K. S., Freedman, E. A., McGarrity, C. T., & Evans, D. C. (2013). *Glishades ericksoni*', an indeterminate juvenile hadrosaurid from the Two Medicine Formation of Montana: implications for hadrosauroid diversity in the latest Cretaceous (Campanian-Maastrichtian) of western North America. *Palaeobiodiversity and Palaeoenvironments*, *93*, 65–75.

Clyde, W. C., Ramezani, J., Johnson, K. R., Bowring, S. A., & Jones, M. M. (2016). Direct high-precision U–Pb geochronology of the end-Cretaceous extinction and calibration of Paleocene astronomical timescales. *Earth and Planetary Science Letters*, *452*, 272–280. doi:10.1016/j.epsl.2016.07.041

Cope, E. D. (1875). Systematic Catalogue of Vertebrata of the Eocene of New Mexico: Collected in 1874. *Report to the Engineer Department*. U.S. Army, U.S. Government Printing Office, Washington, D.C.

Cossette, A. P., & Brochu, C. A. (2020). A systematic review of the giant alligatoroid *Deinosuchus* from the Campanian of North America and its implications for the relationships at the root of Crocodylia. *Journal of Vertebrate Paleontology*, *40*(1), e1767638. doi:10.1080/02724634.2020.1767638

Cossette, A. P., Grass, A. D., & DeGuzman, T. (2022). The contribution of ontogenetic growth trajectories on the divergent evolution of the crocodylian skull table. *The Anatomical Record*, *305*(10), 2904–2925. doi:10.1002/ar.24824

Dahlberg, E. L., Eberle, J. J., Sertich, J. J., & Miller, I. M. (2016). A new earliest Paleocene (Puercan) mammalian fauna from Colorado's Denver Basin, USA. *Rocky Mountain Geology*, *51*(1), 1–22. doi:10.2113/gsrocky.51.1.1

de Araújo Júnior, H. I., & da Silva Marinho, T. (2013). Taphonomy of a *Baurusuchus* (Crocodyliformes, Baurusuchidae) from the Adamantina Formation (Upper Cretaceous, Bauru Basin), Brazil: implications for preservational modes, time resolution and paleoecology. *Journal of South American Earth Sciences*, *47*, 90–99. doi:10.1016/j.jsames.2013.07.006

De Buffrénil, V., Clarac, F., Fau, M., Martin, S., Martin, B., Pellé, E., & Laurin, M. (2015). Differentiation and growth of bone ornamentation in vertebrates: a comparative histological study among the Crocodylomorpha. *Journal of Morphology*, *276*(4), 425–445. doi:10.1002/jmor.20351

De Celis, A., Narváez, I., & Ortega, F. (2020). Spatiotemporal palaeodiversity patterns of modern crocodiles (Crocodyliformes: Eusuchia). *Zoological Journal of the Linnean Society*, *189*(2), 635–656. doi:10.1093/zoolinnean/zlz038

Delfino, M., & Smith, T. (2012). Reappraisal of the morphology and phylogenetic relationships of the middle Eocene alligatoroid *Diplocynodon deponiae* (Frey, Laemmert, and Riess, 1987) based on a three-dimensional specimen. *Journal of Vertebrate Paleontology*, *32*(6), 1358–1369. doi:10.1080/02724634.2012.699484

Delfino, M., Codrea, V., Folie, A., Dica, P., Godefroit, P., & Smith, T. (2008). A complete skull of *Allodaposuchus precedens* Nopcsa, 1928 (Eusuchia) and a reassessment of the morphology of the taxon based on the Romanian remains. *Journal of Vertebrate Paleontology*, *28*(1), 111–122. doi:10.1671/0272-4634(2008)28[111:ACSOAP]2.0.CO;2

Delfino, M., Piras, P., & Smith, T. (2005). Anatomy and phylogeny of the gavialoid crocodylian *Eusuchus lerichei* from the Paleogene of Europe. *Acta Palaeontologica Polonica*, *50*, 565–580.

Erickson, B. R. (1972). The lepidosaurian reptile *Champsosaurus* in North America. *Monographs of the Science Museum of Minnesota (Paleontology)*, *1*, 1–91. doi:10.1159/000393353

Erickson, B. R. (1976). Osteology of the early eusuchian crocodile *Leidyosuchus formidabilis*, sp. nov. *Monographs of the Science Museum of Minnesota (Paleontology)*, *2*, 1–61.

Farke, A. A., Henn, M. M., Woodward, S. J., & Xu, H. A. (2014). *Leidyosuchus* (Crocodylia: Alligatoroidea) from the Upper Cretaceous Kaiparowits Formation (late Campanian) of Utah, USA. *PaleoBios*, *30*(3). doi:10.5070/P9303016247

Farlow, J. O., Hurlburt, G. R., Elsey, R. M., Britton, A. R., & LangstonJrW. (2005). Femoral dimensions and body size of *Alligator mississippiensis*: estimating the size of extinct mesoeucrocodylians. *Journal of Vertebrate Paleontology*, *25*(2), 354–369. doi:10.1671/0272-4634(2005)025[0354:FDABSO]2.0.CO;2

Feijó, A., Karlsson, C. M., Gray, R., Yang, Q., & Hughes, A. C. (2023). Extreme-sized anurans are more prone to climate-driven extinctions. *Climate Change Ecology*, *4*, 100062. doi:10.1016/j.ecochg.2022.100062

Field, D. J., Bercovici, A., Berv, J. S., Dunn, R., Fastovsky, D. E., Lyson, T. R., … Gauthier, J. A. (2018). Early evolution of modern birds structured by global forest collapse at the end-Cretaceous mass extinction. *Current Biology*, *28*(11), 1825–1831. doi:10.1016/j.cub.2018.04.062

Figueiredo, R. G., Moreira, J. K., Saraiva, A. A., & Kellner, A. W. (2011). Description of a new specimen of *Susisuchus anatoceps* (Crocodylomorpha: Mesoeucrocodylia) from the Crato Formation (Santana Group) with comments on Neosuchia. *Zoological Journal of the Linnean Society*, *163*(suppl_1), S273–S288. doi:10.1111/j.1096-3642.2011.00721.x

Fuentes, A. J., Clyde, W. C., Weissenburger, K., Bercovici, A., Lyson, T. R., Miller, I. M., … Johnson, K. R. (2019). Constructing a time scale of biotic recovery across the Cretaceous–Paleogene boundary, Corral Bluffs, Denver Basin, Colorado, USA. *Rocky Mountain Geology*, *54*(2), 133–153. doi:10.24872/rmgjournal.54.2.133

Gilmore, C. W. (1910). *Leidyosuchus sternbergii*, a new species of crocodile from the Cretaceous Beds of Wyoming. *Proceedings of the United States National Museum*, *38*(1762), 485–502. doi:10.5479/si.00963801.38-1762.485

Gmelin, J. F. (1789). Amphibia. *Croli a Linnè Systema naturae* (13 ed. Vol. 1. pp. 1033-1516). G. E. Beer, Lipsiae.

Goloboff, P. A., & Morales, M. E. (2023). TNT version 1.6, with a graphical interface for MacOS and Linux, including new routines in parallel. *Cladistics*.

Goloboff, P. A., Torres, A., & Arias, J. S. (2018). Weighted parsimony outperforms other methods of phylogenetic inference under models appropriate for morphology. *Cladistics*, *34*(4), 407–437. doi:10.1111/cla.12205

Grange, D. R., & Benton, M. J. (1996). Kimmeridgian metriorhynchid crocodiles from England. *Palaeontology*, *39*, 497–514.

Hagadorn, J. W., Bercovici, A., Fleming, R. F., Whiteley, K. R., Yusas, M. R., Lyson, T. R., & Henderson, C. M. (2023). Palynology of Permian red-bed successions of Colorado and Wyoming and its influence on Laramide strata. *Rocky Mountain Geology*, *58*(1), 1–17. doi:10.24872/rmgjournal.58.1.1

Harris, W. H. (2015). Ontogenesis in the cranium of *Alligator mississippiensis* based on disarticulated cranial elements. (Master's thesis, East Tennessee State University).

Hastings, A. K., Reisser, M., & Scheyer, T. M. (2016). Character evolution and the origin of Caimaninae (Crocodylia) in the New World Tropics: new evidence from the Miocene of Panama and Venezuela. *Journal of Paleontology*, *90*(2), 317–332. doi:10.1017/jpa.2016.37

Hekkala, E., Gatesy, J., Narechania, A., et al. (2021). Paleogenomics illuminates the evolutionary history of the extinct Holocene "horned" crocodile of Madagascar, *Voay robustus*. *Communications Biology*, *4*(1), 505. doi:10.1038/s42003-021-02017-0

Hester, D. A. (2018). A review of the Paleogene eusuchian crocodyliform *Borealosuchus wilsoni* (Mook, 1959) from western North America (Doctoral dissertation, The University of Iowa).

Huxley, T. H. (1875). On *Stagonolepis robertsoni*, and on the evolution of the Crocodilia. *Quarterly Journal of the Geological Society of London*, *31*(1-4), 423–438. doi:10.1144/GSL.JGS.1875.031.01-04.29

Iijima, M., & Kubo, T. (2020). Vertebrae-based body length estimation in crocodylians and its implication for sexual maturity and the maximum sizes. *Integrative Organismal Biology*, *2*(1), obaa042. doi:10.1093/iob/obaa042

Iijima, M., Kubo, T., & Kobayashi, Y. (2018). Comparative limb proportions reveal differential locomotor morphofunctions of alligatoroids and crocodyloids. *Royal Society open science*, *5*(3), 171774. doi:10.1098/rsos.171774

Joyce, W. G., Brinkman, D., & Lyson, T. R. (2019). A new species of trionychid turtle, *Axestemys infernalis sp. nov.*, from the Late Cretaceous (Maastrichtian) Hell Creek and Lance formations of the Northern Great Plains, USA. *Palaeontologia Electronica, 22.3.72*, 1–28.

Krause, D. W., Hoffmann, S., Lyson, T. R., Dougan, L. G., Petermann, H., Tecza, A., … Miller, I. M. (2021). New skull material of *Taeniolabis taoensis* (Multituberculata, Taeniolabididae) from the early Paleocene (Danian) of the Denver Basin, Colorado. *Journal of Mammalian Evolution*, *28*(4), 1083–1143. doi:10.1007/s10914-021-09584-3

Lessner, E. J., & Holliday, C. M. (2022). A 3D ontogenetic atlas of *Alligator mississippiensis* cranial nerves and their significance for comparative neurology of reptiles. *The Anatomical Record*, *305*(10), 2854–2882. doi:10.1002/ar.24550

Lindblad, K. T., Moreno-Bernal, J. W., McKellar, R. C., & Velez, M. I. (2022). The Northern Crocodile: first report of Borealosuchus (Eusuchia; Crocodylia) from Saskatchewan's lower Ravenscrag Formation (earliest Paleocene) with implications for biogeography. *Canadian Journal of Earth Sciences*, *59*(9), 623–638. doi:10.1139/cjes-2022-0010

Lucas, S. G. (1988). Eocene Crocodilia from the San Jose Formation, San Juan Basin, New Mexico. *New Mexico Journal of Science*, *28*(2), 93–98.

Lucas, S. G., & Sullivan, R. M. (1986). *Leidyosuchus* (Reptilia, Crocodilia) from the Paleocene Nacimiento Formation, San Juan Basin, New Mexico. *New Mexico Journal of Science*, *26*(2), 31–38.

Lyson, T. R., Miller, I. M., Bercovici, A. D., Weissenburger, K., Fuentes, A. J., Clyde, W. C., … Chester, S. G. B. (2019). Exceptional continental record of biotic recovery after the Cretaceous–Paleogene mass extinction. *Science*, *366*(6468), 977–983. doi:10.1126/science.aay2268

Lyson, T. R., Petermann, H., & Miller, I. M. (2021a). A new plastomenid trionychid turtle, *Plastomenus joycei, sp. nov.*, from the earliest Paleocene (Danian) Denver Formation of south-central Colorado, USA. *Journal of Vertebrate Paleontology*, *41*(1), e1913600. doi:10.1080/02724634.2021.1913600

Lyson, T. R., Petermann, H., Toth, N., Bastien, S., & Miller, I. M. (2021b). A new baenid turtle, *Palatobaena knellerorum sp. nov.*, from the lower Paleocene (Danian) Denver Formation of south-central Colorado, USA. *Journal of Vertebrate Paleontology*, *41*(2), e1925558. doi:10.1080/02724634.2021.1925558

MacLeod, N., Rawson, P. F., Forey, P. L., Banner, F. T., Boudagher-Fadel, M. K., Bown, P. R., … Young, J. R. (1997). The Cretaceous-tertiary biotic transition. *Journal of the Geological Society*, *154*(2), 265–292. doi:10.1144/gsjgs.154.2.0265

Maddison, W. P., & Maddison, D. R. (2023). Mesquite: a modular system for evolutionary analysis. Version 3.81 http://www.mesquiteproject.org.

Markwick, P. J. (1998). Crocodilian diversity in space and time: the role of climate in paleoecology and its implication for understanding K/T extinctions. *Paleobiology*, *24*(4), 470–497. doi:10.1017/S009483730002011X

Martin, J. E., Smith, T., de Lapparent de Broin, F., Escuillié, F., & Delfino, M. (2014). Late Palaeocene eusuchian remains from Mont de Berru, France, and the origin of the alligatoroid Diplocynodon. *Zoological Journal of the Linnean Society*, *172*(4), 867–891. doi:10.1111/zoj.12195

McCormack, L. (2019). *Borealosuchus* (Crocodylia) from the early Campanian Mooreville chalk reveals new insights into the Late Cretaceous fauna of Alabama and the origin of Crocodylian lineages (Doctoral dissertation, The University of Iowa).

Middleton, M. D. (1983). *Early Paleocene vertebrates of the Denver Basin, Colorado*. University of Colorado at Boulder.

Mook, C. C. (1921). Individual and age variations in the skulls of recent Crocodilia. *Bulletin of the American Museum of Natural History*, *44*, 51.

Mook, C. C. (1959). A new species of fossil crocodile of the genus *Leidyosuchus* from the Green River Beds. *American Museum Novitiates*, 1933, 1-6.

Narváez, I., Brochu, C. A., Escaso, F., Pérez-García, A., & Ortega, F. (2015). New crocodyliforms from southwestern Europe and definition of a diverse clade of European Late Cretaceous basal eusuchians. *PLoS ONE*, *10*(11), e0140679. doi:10.1371/journal.pone.0140679

Nichols, D. J., & Fleming, R. F. (2002). Palynology and palynostratigraphy of Maastrichtian, Paleocene, and Eocene strata in the Denver Basin, Colorado. *Rocky Mountain Geology*, *37*(2), 135–163. doi:10.2113/gsrocky.37.2.135

Nixon, K. C. (2021). *ASADO, version 2.0*. Published by the author.

O'Brien, H. D., Lynch, L. M., Vliet, K. A., Brueggen, J., Erickson, G. M., & Gignac, P. M. (2019). Crocodylian head width allometry and phylogenetic prediction of body size in extinct crocodyliforms. *Integrative Organismal Biology*, *1*(1), obz006.

Obasi, C. C., TerryJrD. O., Myer, G. H., & Grandstaff, D. E. (2011). Glauconite composition and morphology, shocked quartz, and the origin of the Cretaceous (?) Main Fossiliferous Layer (MFL) in southern New Jersey, USA. *Journal of Sedimentary Research*, *81*(7), 479–494. doi:10.2110/jsr.2011.42

Petermann, H., Lyson, T. R., Miller, I. M., & Hagadorn, J. W. (2022). Crushed turtle shells: Proxies for lithification and burial-depth histories. *Geosphere*, *18*(5), 1524–1537. doi:10.1130/GES02513.1

Pol, D., Turner, A. H., & Norell, M. A. (2009). Morphology of the Late Cretaceous crocodylomorph *Shamosuchus djadochtaensis* and a discussion of neosuchian phylogeny as related to the origin of Eusuchia. *Bulletin of the American Museum of Natural History*, *2009*(324), 1–103.

Puértolas, E., Canudo, J. I., & Cruzado-Caballero, P. (2011). A new crocodylian from the Late Maastrichtian of Spain: implications for the initial radiation of crocodyloids. *PLoS ONE*, *6*(6), e20011. doi:10.1371/journal.pone.0020011

Raynolds, R. G. (2002). Upper Cretaceous and Tertiary stratigraphy of the Denver basin, Colorado. *Rocky Mountain Geology*, *37*(2), 111–134. doi:10.2113/gsrocky.37.2.111

Raynolds, R. G., & Johnson, K. R. (2003). Synopsis of the stratigraphy and paleontology of the uppermost Cretaceous and lower Tertiary strata in the Denver Basin, Colorado. *Rocky Mountain Geology*, *38*(1), 171–181. doi:10.2113/gsrocky.38.1.171

Rio, J. P., & Mannion, P. D. (2021). Phylogenetic analysis of a new morphological dataset elucidates the evolutionary history of

Crocodylia and resolves the long-standing gharial problem. *PeerJ*, *9*, e12094. doi:10.7717/peerj.12094

Robertson, D. S., McKenna, M. C., Toon, O. B., Hope, S., & Lillegraven, J. A. (2004). Survival in the first hours of the Cenozoic. *Geological Society of America Bulletin*, *116*(5-6), 760–768. doi:10.1130/B25402.1

Salisbury, S. W., Frey, E., Martill, D. M., & Buchy, M. C. (2003). A new crocodilian from the Lower Cretaceous Crato Formation of north-eastern Brazil. *Palaeontographica Abteilung A*, *270*(1-3), 3–47. doi:10.1127/pala/270/2003/3

Schwarz-Wings, D., Klein, N., Neumann, C., & Resch, U. (2011). A new partial skeleton of *Alligatorellus* (Crocodyliformes) associated with echinoids from the Late Jurassic (Tithonian) lithographic limestone of Kelheim, S-Germany. *Fossil Record*, *14*(2), 195–205. doi:10.5194/fr-14-195-2011

Sternberg, C. M. (1932). A new fossil crocodile from Saskatchewan. *The Canadian Field-Naturalist*, *44*(6), 128–133. doi:10.5962/p.339381

Stout, J. B. (2012). New material of *Borealosuchus* from the Bridger Formation, with notes on the paleoecology of Wyoming's Eocene crocodylians. *PalArch's Journal of Vertebrate Palaeontology*, *9*(5).

Sullivan, R. M. (1987). A reassessment of reptilian diversity across the Cretaceous-Tertiary boundary. *Contributions in science. Natural history museum of Los Angeles County*, 391.

Syme, C. E., & Salisbury, S. W. (2014). Patterns of aquatic decay and disarticulation in juvenile Indo-Pacific crocodiles (*Crocodylus porosus*), and implications for the taphonomic interpretation of fossil crocodyliform material. *Palaeogeography, Palaeoclimatology, Palaeoecology*, *412*, 108–123. doi:10.1016/j.palaeo.2014.07.031

Tsuihiji, T., Watabe, M., Tsogtbaatar, K., Tsubamoto, T., Barsbold, R., Suzuki, S., … Witmer, L. M. (2011). Cranial osteology of a juvenile specimen of *Tarbosaurus bataar* (Theropoda, Tyrannosauridae) from the Nemegt Formation (Upper Cretaceous) of Bugin Tsav, Mongolia. *Journal of Vertebrate Paleontology*, *31*(3), 497–517. doi:10.1080/02724634.2011.557116

Voegele, K. K., Ullmann, P. V., Lonsdorf, T., Christman, Z., Heierbacher, M., Kibelstis, B. J., … Lacovara, K. J. (2021). Microstratigraphic analysis of fossil distribution in the lower Hornerstown and upper Navesink formations at the Edelman Fossil Park, NJ. *Frontiers in Earth Science*, *9*, 756655. doi:10.3389/feart.2021.756655

Watanabe, A., Gignac, P. M., Balanoff, A. M., Green, T. L., Kley, N. J., & Norell, M. A. (2019). Are endocasts good proxies for brain size and shape in archosaurs throughout ontogeny? *Journal of Anatomy*, *234*(3), 291–305. doi:10.1111/joa.12918

Weaver, L. N., Crowell, J. W., Chester, S. G. B., & Lyson, T. R. (2024). Skull of a new periptychid mammal from the lower Paleocene Denver Formation of Colorado (Corral Bluffs, El Paso County). *Journal of Mammalian Evolution*, *31*(2), 1–26. doi:10.1007/s10914-024-09716-5

Williams, S. A., Brochu, C. A., Tremaine, K. M., Carr, R., Varricchio, D. J., & Scanella, J. (2018). First occurrence of *Borealosuchus* and other crocodyliform fossil material from the Upper Cretaceous Two Medicine Formation of Northwestern Montana. *Journal of Vertebrate Paleontology*, *B91*.

Wilson, G. P. (2013). Mammals across the K/Pg boundary in northeastern Montana, USA: dental morphology and body-size patterns reveal extinction selectivity and immigrant-fueled ecospace filling. *Paleobiology*, *39*(3), 429–469. doi:10.1666/12041

Wu, X. C., & Brinkman, D. B. (2015). A new crocodylian (Eusuchia) from the uppermost Cretaceous of Alberta, Canada. *Canadian Journal of Earth Sciences*, *52*(8), 590–607. doi:10.1139/cjes-2014-0133

Wu, X. C., Brinkman, D. B., & Fox, R. C. (2001). A new crocodylian (Archosauria) from the basal Paleocene of the Red Deer River Valley, southern Alberta. *Canadian Journal of Earth Sciences*, *38*(12), 1689–1704. doi:10.1139/e01-052

Handling Editor: Pedro Godoy.
Phylogenetics Editor: Pedro Godoy.